TISSUE ENGINEERING: Part C
Volume 16, Number 3, 2010

DOI: 10.1089/ten.tec.2009.0362

Cardiomyoblast-like Cells Differentiated from Human Adipose Tissue-Derived Mesenchymal Stem Cells Improve Left Ventricular Dysfunction and Survival in a Rat Myocardial Infarction Model

Hanayuki Okura, M.S.,[1–4] Akifumi Matsuyama, M.D., Ph.D.,[1] Chun-Man Lee, M.D., Ph.D.,[1,2] Ayami Saga, M.S.,[1] Aya Kakuta-Yamamoto, B.S.,[1] Anna Nagao, B.S.,[1,2] Nagako Sougawa, D.M.D., Ph.D.,[1] Naosumi Sekiya, M.D.,[3] Kazuhiro Takekita, M.S.,[1,2] Yashuhiro Shudo, M.D.,[3] Shigeru Miyagawa, M.D., Ph.D.,[3] Hiroshi Komoda, M.D., Ph.D.,[1,5] Teruo Okano, Ph.D.,[6] and Yoshiki Sawa, M.D., Ph.D.[2,3]

Adipose tissue–derived mesenchymal stem cells (ADMSCs) are multipotent cells. Here we examined whether human ADMSCs (hADMSCs) could differentiate into cardiomyoblast-like cells (CLCs) by induction with dimethylsulfoxide and whether the cells would be utilized to treat cardiac dysfunction. Dimethylsulfoxide induced the expression of various cardiac markers in hADMSCs, such as α-cardiac actin, cardiac myosin light chain, and myosin heavy chain; none of which were detected in noncommitted hADMSCs. The induced cells were thus designated as hADMSC-derived CLCs (hCLCs). To confirm their beneficial effect on cardiac function, hCLC patches were transplanted onto the Nude rat myocardial infarction model, and compared with noncommitted hADMSC patch transplants and sham operations. Echocardiography demonstrated significant short-term improvement of cardiac function in both the patch-transplanted groups. However, long-term follow-up showed rescue and maintenance of cardiac function in the hCLC patch-transplanted group only, but not in the noncommitted hADMSC patch-transplanted animals. The hCLCs, but not the hADMSCs, engrafted into the scarred myocardium and differentiated into human cardiac troponin I-positive cells, and thus regarded as cardiomyocytes. Transplantation of the hCLC patches also resulted in recovery of cardiac function and improvement of long-term survival rate. Thus, transplantation of hCLC patches is a potentially effective therapeutic strategy for future cardiac tissue regeneration.

Introduction

END-STAGE HEART FAILURE remains a major cause of death worldwide, with most cases due to ischemia. This is despite the remarkable progress in recent years in both medical and surgical treatments for heart failure. Cardiac transplantation and mechanical support using implantation of the left ventricular assist system were established as the ultimate means of support for these patients.[1,2] However, these treatment entities have limitations including donor shortage, rejection, and left ventricular assist system durability, and alternative strategies are needed in such circumstances.

Cellular cardiomyoplasty was developed as a new approach to restore impaired heart function,[3,4] using a variety of cell types, with encouraging initial results.[3–5] Mesenchymal stem cells (MSCs) seem particularly advantageous for cellular therapy in general because they are multipotent, potentially immune privileged,[6] and expand easily *ex vivo*. MSCs also proliferate rapidly, induce angiogenesis, and can differentiate into cardiomyogenic cells.[7–10] An MSC population was recently isolated from human adipose tissue, which is abundantly available and can be resected easily and safely in most patients.[11,12] These adipose tissue-derived cell lineages showed cardiomyocytic differentiation and rescued

[1]Department of Somatic Stem Cell Therapy, Foundation for Biomedical Research and Innovation, Kobe, Japan.
[2]Medical Center for Translational Research, Osaka University Hospital, Suita, Japan.
[3]Department of Surgery, Osaka University Graduate School of Medicine, Suita, Japan.
[4]Research Fellow of the Japan Society for the Promotion of Science, Tokyo, Japan.
[5]Department of Internal Medicine, National Hospital Organization Chiba Medical Center, Chiba, Japan.
[6]Institute of Advanced Biomedical Engineering and Science, Tokyo Women's Medical University, Tokyo, Japan.

cardiac dysfunction in a myocardial infarction (MI) animal model. Thus, the adipose tissue is a convenient and preferred source of stem cell recovery for cardiac therapy. Recently, transplantation of monolayered adipose tissue-derived MSCs (ADMSCs) into MI rats reversed wall thinning in the scarred area and improved cardiac function in a short term, with the engrafted sheet of cells forming a thick stratum containing newly formed vessels and scattered cardiomyocytes derived from the implanted cells.[13] As patients with severe heart failure desire sustained and long-term recovery of cardiac function after treatment rather than short-term improvement, continued efforts should be made to develop cell transplants from ADMSCs that survive and differentiate into cardiomyocytes *in vivo* for subsequent engraftment onto scarred myocardium.

This study investigated the differentiation of human ADMSCs (hADMSCs) into cardiomyoblast-like cells (CLCs) *in vitro*, analyzed the functional and histological regeneration of damaged myocardium after transplantation of CLCs *in vivo*, and examined the effects of such transplantation on long-term patient survival.

Materials and Methods

Adipose tissues from human subjects

Excess omental adipose tissues were resected from the gastro-omental artery during coronary artery bypass graft surgery and gastrectomy in 10 subjects [4 men and 6 women; age, 55 ± 5 years, mean ± standard error of mean (SEM); range, 40–60 years]. All subjects provided informed consent, and the Review Board for Human Research of Osaka University Graduate School of Medicine approved all protocols. All subjects fasted for at least 10 h before surgery and none was on steroid therapy at the time of surgery. Ten to 50 grams of adipose tissue was obtained from each subject.

Isolation of hADMSCs and differentiation into CLCs

hADMSCs were obtained as reported previously, with modification.[11,14] Briefly, the resected excess adipose tissue was minced and then digested at 37°C for 1 h in Hank's balanced salt solution (Gibco–Invitrogen, Grand Island, NY) containing 0.075% collagenase type II (Sigma–Aldrich, St. Louis, MO). Digests were filtered through a cell strainer (BD Bioscience, San Jose, CA) and centrifuged at 800 *g* for 10 min. Red blood cells were excluded using density gradient centrifugation with Lymphoprep ($d = 1.077$; Nycomed, Oslo, Norway), and the remaining cells were cultured in Dulbecco's modified Eagle's medium (Gibco–Invitrogen) with 10% defined fetal bovine serum (Hyclone, Logan, UT) for 24 h at 37°C. Following incubation, the adherent cells were washed extensively and then treated with 0.2 g/L ethylenediaminetetraacetate solution (Nacalai Tesque, Kyoto, Japan). The resulting suspended cells were replated at a density of 10,000 cells/cm^2 on human fibronectin-coated dishes (BD BioCoat, Franklin Lakes, NJ) in 60% Dulbecco's modified Eagle's medium-low glucose, 40% MCDB-201 medium (Sigma–Aldrich), 1×insulin-transferring selenium (Gibco–Invitrogen), 1 nM dexamethasone (Sigma–Aldrich), 100 μM ascorbic acid 2-phosphate (Sigma–Aldrich), 10 ng/mL epidermal growth factor (PeproTec, Rocky Hill, NJ), and 5% fetal bovine serum. After passaging five to six times in the same medium, the hADMSCs were used for transplantation. Cardiomyocytic differentiation was achieved by inducing hADMSCs with 0.1% dimethylsulfoxide (DMSO) for 48 h, resulting in a population named CLCs.

Reverse transcriptase–polymerase chain reaction

Total RNA was isolated from hADMSCs and cardiomyoblasts using an RNAeasy kit (Qiagen, Hilden, Germany). As a control, excess human myocardium was resected during maze surgery from 10 matched subjects (4 men and 6 women; age, 55 ± 5 years, mean ± SEM; range, 40–60 years) with informed consent. Control subjects also fasted for at least 10 h before surgery, and none was taking steroids. Approximately 1 g of myocardium was obtained from each subject, and the same protocol was performed to obtain total RNA. After treatment with DNase, cDNA was synthesized from 500 ng total RNA using Superscript III reverse transcriptase RNase H minus (Invitrogen, Carlsbad, CA). The absence of DNA contamination in RNA samples was confirmed with polymerase chain reaction (PCR) primers flanking an intron. Primers and the reaction conditions are described in Table 1. The PCR products were fractionated by 2% agarose gel electrophoresis.

Table 1. Primers Used in Reverse Transcriptase–Polymerase Chain Reaction

Primer		*Sequence*	*No. of cycles*	*Annealing temperature (°C)*
GAPDH	Forward	GTCAGTGGTGGACCTGACCT	35	60
	Reverse	AGGGGAGATTCAGTGTGGTG		
Islet-1	Forward	TGATGAAGCAACTCCAGCAG	35	60
	Reverse	GGACTGGCTACCATGCTGTT		
Nkx2.5	Forward	GGTGGAGCTGGAGAAGACAGA	35	60
	Reverse	CGACGCCGAAGTTCACGAAGT		
GATA-4	Forward	ACCAGCAGCAGCGAGGAGAT	35	60
	Reverse	GAGAGATGCAGTGTGCTCGT		
α-Cardiac actin	Forward	GGAGTTATGGTGGGTATGGGTC	35	60
	Reverse	AGTGGTGACAAAGGAGTAGCCA		
Myosin light chain-2v	Forward	5′-GCGCCAACTCCAACGTGTTCT	35	60
	Reverse	5′-GTGATGATGTGCACCAGGTTC		
Myosin heavy chain	Forward	GGGGACAGTGGTAAAAGCAA	35	60
	Reverse	TCCCTGCGTTCCACTATCTT		

Model animals for MI

The left anterior descending coronary artery of rats with severe combined immunodeficiency was ligated. In brief, rats were anesthetized with nembutal (40 mg/kg), before being intubated and ventilated at a rate of 60 cycles/min with a tidal volume of 5 mL under room air supplemented with oxygen (2 L/min). The hearts were exposed through the fifth left-intercostal space and the left anterior descending was ligated. After 4 weeks, the hearts were again exposed through the fifth left-intercostal space, and the infarct area was identified visually based on surface scarring and abnormal wall motion. Cell sheets were subsequently implanted onto the infarcted myocardium. The control group was treated similarly, but no cell sheets were implanted. The Osaka University Graduate School of Medicine Standing Committee on Animals approved all experimental protocols.

Preparation of monolayered cell sheets

After four to five passages, the hADMSCs were trypsinized and then replated onto 35-mm temperature-responsive dishes (CellSeed, Tokyo, Japan) in 2 mL of expansion medium at 1×10^6 cells per dish. After culture at 37°C for 2 days, 0.1% DMSO was added to the medium on half of the dishes to differentiate the hADMSCs into cardiomyoblasts. After 2 days of culture, the cells were incubated again at 20°C. Within 20 min, the hADMSCs and CLC sheets detached spontaneously and floated up into the medium for use as monolayered cell grafts.[13,15–17]

Assessment of rat cardiac function

Cardiac ultrasound studies were performed before ligation, before implantation, and at 2, 4, 8, 10, 12, 14, and 16 weeks after implantation using a SONOS 7500 (Philips Medical Systems, Andover, MA). Plasma atrial natriuretic protein (ANP) level was analyzed using an ANP ELISA system (Phoenix Pharmaceuticals, Burlingame, CA) by following the instructions supplied by the manufacturer.

Histological analyses

The rat hearts were dissected out and immediately fixed overnight in 4% paraformaldehyde, washed in 70% alcohol, dehydrated through a graded ethanol series, cleared in xylene, and finally processed for embedding in paraffin wax. Paraffin sections were cut at 5 μm thickness, delineated on the microscope slide using a Dako pen (Dako, Glostrup, Denmark), deparaffinized in xylene, and then rehydrated through a graded ethanol series into distilled water. The sections were then immersed in Target Retrieval Solution (Dako) in distilled water and boiled, followed by cooling at room temperature for 20 min. The sections were then washed in two changes of Tris-buffered saline (TBS), pH 7.4, followed by 1% polyoxyethylene sorbitan monolaurate (Tween 20) in TBS (TBS-T), and then an overnight incubation with 10% Blocking One® (Nacalai Tesque) in TBS-T. The sections were then incubated in a humid chamber for 16 h at 4°C with mouse monoclonal antibodies to α-cardiac actin (α-CA) and human troponin I, diluted in the blocking solution, followed by Alexa Fluor 546-labeled donkey anti-goat IgG (Molecular Probes, Eugene, OR). The stained slides were viewed on a BioZero laser scanning microscope (Keyence, Osaka, Japan).

Statistical analysis

All data were expressed as mean ± SEM. Differences between groups were analyzed for statistical significance by the Student's *t*-test using SPSS Statistics 17.0 (SPSS, Inc., Chicago, IL). A *p*-value less than 0.05 denoted a statistically significant difference. Survival curves were constructed by the Kaplan–Meier method and survival among groups was compared using the Log-Rank test (StatMate III for Windows; Atoms, Tokyo, Japan).

Results

Cardiac differentiation of hADMSCs into CLCs

The potential for hADMSCs to differentiate into CLCs was evaluated from the mRNA expression of several cardiac differentiation markers by reverse transcriptase-PCR before and after DMSO induction, as follows: *islet-1* is a cardiac stem cell marker; *Nkx2.5* and *GATA-4* are transcription factors required for subsequent cardiac differentiation; and α-*CA*, *myosin light chain*, and *myosin heavy chain* (*MHC*) are markers of cardiac differentiation (Fig. 1A). Preinduced hADMSCs expressed *islet-1* and *Nkx2.5* mRNA, but not that of *GATA-4*, α-*CA*, *myosin light chain*, or *MHC*. After induction by DMSO for 48 h, hADMSCs expressed all markers, indicating that DMSO treatment successfully differentiated hADMSCs into cells of the cardiac lineage, and these induced cells were named CLCs.

Preparation and transplantation of hADMSC-derived CLC patches

To evaluate the potential therapeutic usefulness of CLCs, we designed an experimental rat model of coronary ligated infarction to assess cardiac function after transplantation of CLC patches. CLC and control hADMSC patches were prepared from cell sheets, as described earlier (Fig. 1B). These patches were transplanted onto the scarred area of the left ventricular wall in the MI model Nude rats, whose left anterior descending artery had been ligated 4 weeks before graft implantation (Fig. 1C, D). Sham transplantations were also performed.

Effects of CLC transplantation on cardiac function and survival rate

Cardiac function was assessed by echocardiography at preligation, pretransplantation, and every 2 weeks after transplantation (Fig. 1D). Sixteen weeks after transplantation, the treated animals were sacrificed and cardiac tissues prepared for histological examination. Four weeks after graft implantation, wall motion was improved in both control and CLC patch-implanted hearts. However, the wall motion of control and noncommitted hADMSC patch-transplanted heart tissue was exacerbated at 16 weeks after transplantation, while improved motion was maintained with the CLC patch transplants (Fig. 2A). In the early phases of the post-transplantation period, left ventricular diastolic dimension was significantly reduced in both the transplanted groups, but by 8 weeks after implantation this parameter increased in the control hADMSC patch-transplanted group, whereas it remained unchanged in those animals that received CLC patch transplants (Fig. 2B). Likewise, left ventricular ejection

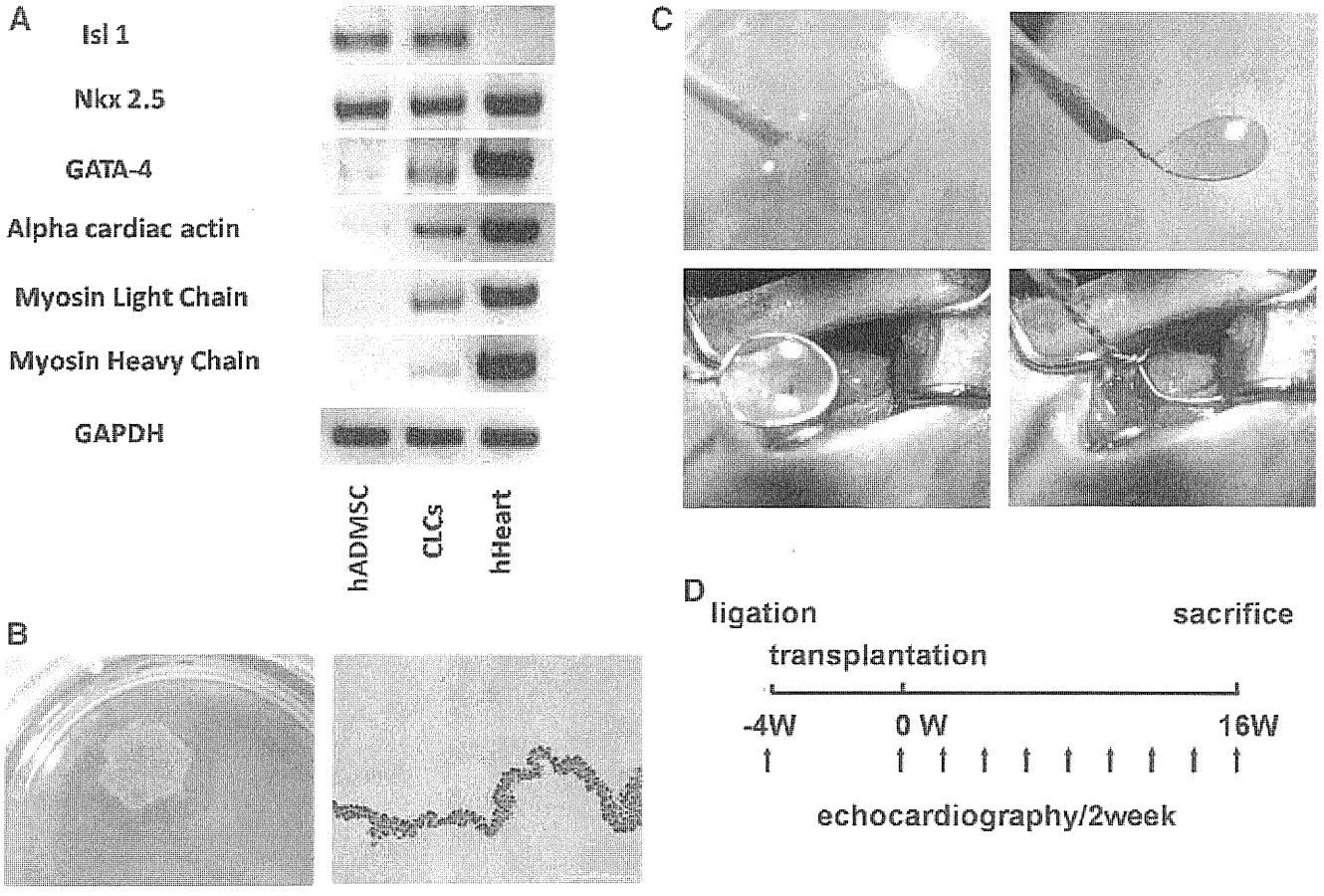

FIG. 1. Preparation and transplantation of human adipose tissue-derived mesenchymal stem cell (hADMSC)-derived cardiomyoblast-like cell (hCLC) patches. (A) Treatment with dimethylsulfoxide (DMSO) transformed hADMSCs into CLCs. The mRNA expressions of *islet-1*, *Nkx2.5*, *GATA-4*, *α-cardiac actin* (*α-CA*), *myosin light chain* (*MLC*), and *MHC* were analyzed by reverse transcriptase–polymerase chain reaction. The mRNAs for *islet-1* and *Nkx2.5*, with trace levels of *GATA-4* and *α-CA*, were expressed in hADMSCs, but no expression of *MLC* or *MHC* was detected. After induction with DMSO for 48 h, the hADMSCs also expressed *MLC* and *MHC*, indicating a phenotypic change into CLCs. (B) Preparation of hADMSC-derived CLC patches. The hADMSCs were cultured on temperature-responsive dishes for 48 h with 0.1% of DMSO for differentiation into CLCs. As the culture temperature was decreased from 37°C to 20°C, the CLCs detached spontaneously as sheets and floated up within 30 min into the culture media as a layered CLC patch. (C) Transplantation of hADMSC-derived CLC patches. Detached patches were transplanted onto the left ventricular wall scar in the myocardial infarction (MI) model Nude rats. (D) Protocol used for assessment of cardiac function. The left anterior descending artery was ligated in Nude rats at 4 weeks before graft implantation. Cardiac function was assessed by echocardiography at preligation, pretransplantation, and every 2 weeks following transplantation. The treated animals were sacrificed 16 weeks after transplantation and prepared for histological examination.

fractions improved in both the implanted groups until 8 weeks, after which time it worsened only in the group transplanted with noncommitted hADMSC patches (Fig. 2B).

ANP was then measured to confirm that chronic heart failure due to MI could be treated by CLC patch transplantation (Fig. 2C). The ANP levels were significantly increased after MI in all groups (Fig. 2C). The sham-operated MI control group showed incremental increases in plasma ANP over the time course of examination, whereas both CLC patch- and hADMSC patch-transplanted animals had low ANP levels until 8 weeks after treatment. However, ANP levels increased subsequently in the hADMSC patch-transplanted group, whereas the CLC patch-transplanted group maintained the improvement in ANP levels.

The Kaplan–Meier survival curve showed higher long-term survival rates in cell patch-transplanted groups than in sham-operated MI controls (Fig. 2D). Notably, no rat died after transplantation of an hADMSC-derived CLC patch. Survival at 16 weeks after surgery was 100% for the CLC group, 80% for the hADMSC group, and 16% for the sham-operated group, with a significant difference between the two transplanted groups. These results suggest that transplantation of hADMSC-derived CLCs has beneficial effect in rats with heart failure induced by MI.

Effects of CLC transplantation on cardiac structure

Cardiac structure was next examined histologically to analyze further the difference between CLC patch- and noncommitted hADMSC patch-transplanted animals in the longer term (Fig. 3). On hematoxylin and eosin and Masson trichrome staining, the sham-transplanted MI control rats

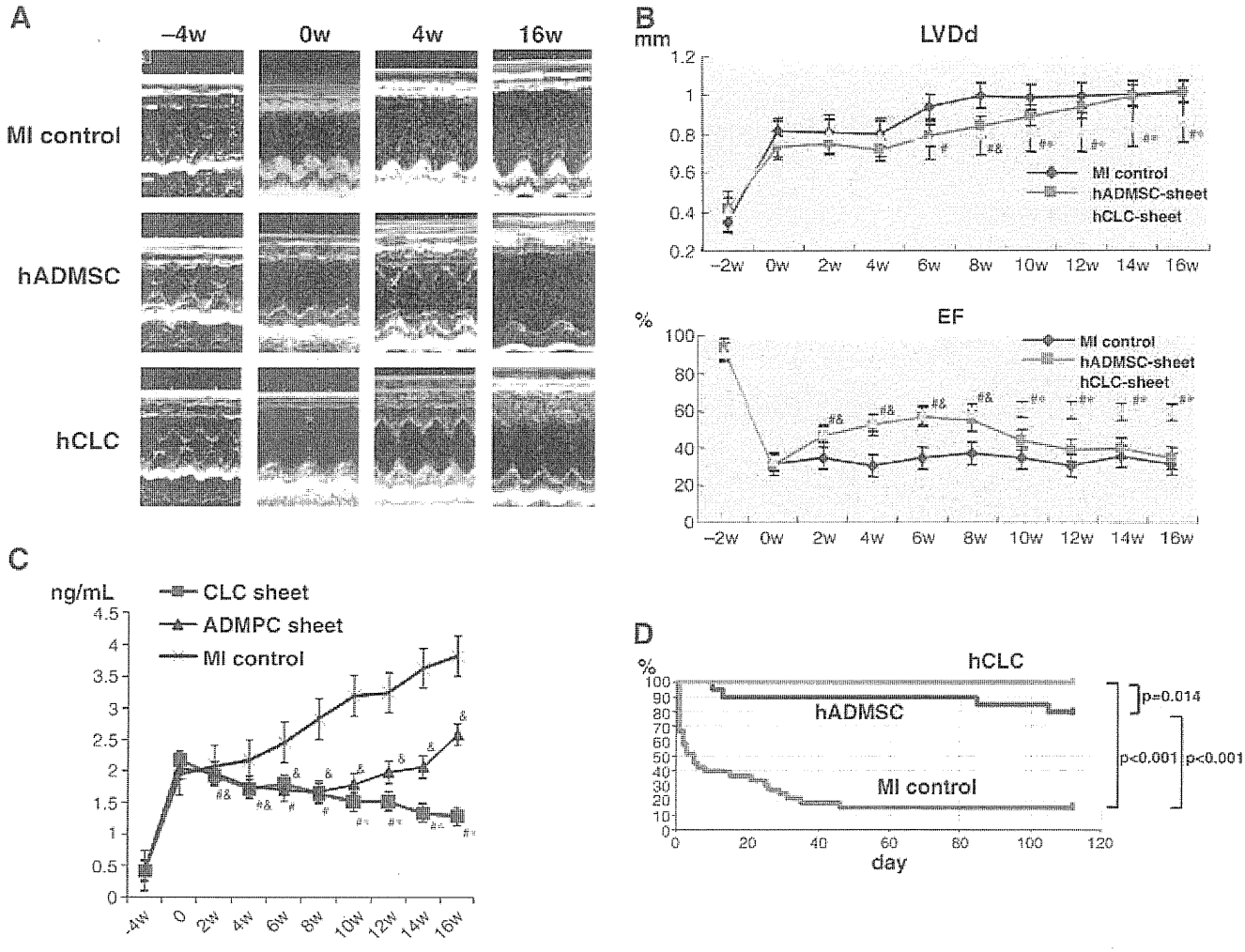

FIG. 2. Effects of CLC patch transplantation on cardiac function and long-term survival. (A) In both the patch-transplanted groups, echocardiography showed improved wall motion within 4 weeks of transplantation. However, at 16 weeks after transplantation, the wall motion of noncommitted hADMSC patch-transplanted rats worsened, whereas it was maintained in the CLC patch-transplanted animals. (B) Left ventricular diastolic dimension and ejection fractions improved significantly in both the patch-grafted groups in the early phase, as confirmed by echocardiography. However, these two parameters of cardiac function worsened at 8 weeks after implantation in the noncommitted hADMSC patch-transplanted groups, but not in the CLC patch-transplanted group. The numbers of all groups were five. Data are mean ± standard error of mean ($^{\#}p < 0.05$; MI control vs. the hCLC patch-transplanted animals; $^{\&}p < 0.05$; MI control vs. the noncommitted-hADMSC patch-transplanted rats; $^{*}p < 0.05$; hCLC patch-transplanted vs. the noncommitted hADMSC patch-transplanted rats, respectively). (C) Plasma ANP levels. Sham-operated MI control group showed increment of plasma ANP levels during the course of the experiment. Both the CLC patch- and hADMSC patch-transplanted groups showed suppression of ANP level increment till 8 weeks after treatment. ANP levels of the hADMSC patch-transplanted group increased from 8 weeks after transplantation, but no change in ANP levels was noted in the CLC patch-transplanted group. The numbers of all groups were four. (D) Long-term survival of rats with chronic heart failure that received the CLC patch ($n = 28$), noncommitted hADMSC patch ($n = 20$), or sham operation ($n = 37$). The Kaplan–Meier survival curve demonstrated that no rat died after transplantation of hADMSC-derived CLC patch. The survival rate at 16 weeks after surgery was 80% for the hADMSC group versus 16% for the sham-operated group. Log-rank test; p-values are indicated. LVDd, left ventricular diastolic dimension.

showed only a thin layer of cardiac muscle and fibrotic tissues in the scarred anterior left ventricular wall (Fig. 3A, B). Rats implanted with noncommitted hADMSCs showed small patches of cardiac muscles over that seen in the control MI rats (Fig. 3C, D). On the other hand, the rats transplanted with CLC patches showed significant reversal of the infracted myocardium and a full cardiac muscle layer overlaying the transplanted area (Fig. 3E, F, arrowheads).

CLCs differentiate into cardiac muscle in situ

The *in situ* differentiation capacity of the implanted cell sheets into cardiomyocytes after grafting onto the scarred myocardium was assessed by immunohistochemical staining for α-CA and human troponin I (Fig. 4). Thin layers of α-CA-positive cells were observed on the scarred myocardium of sham-operated MI control rats (Fig. 4A). A similar but thicker

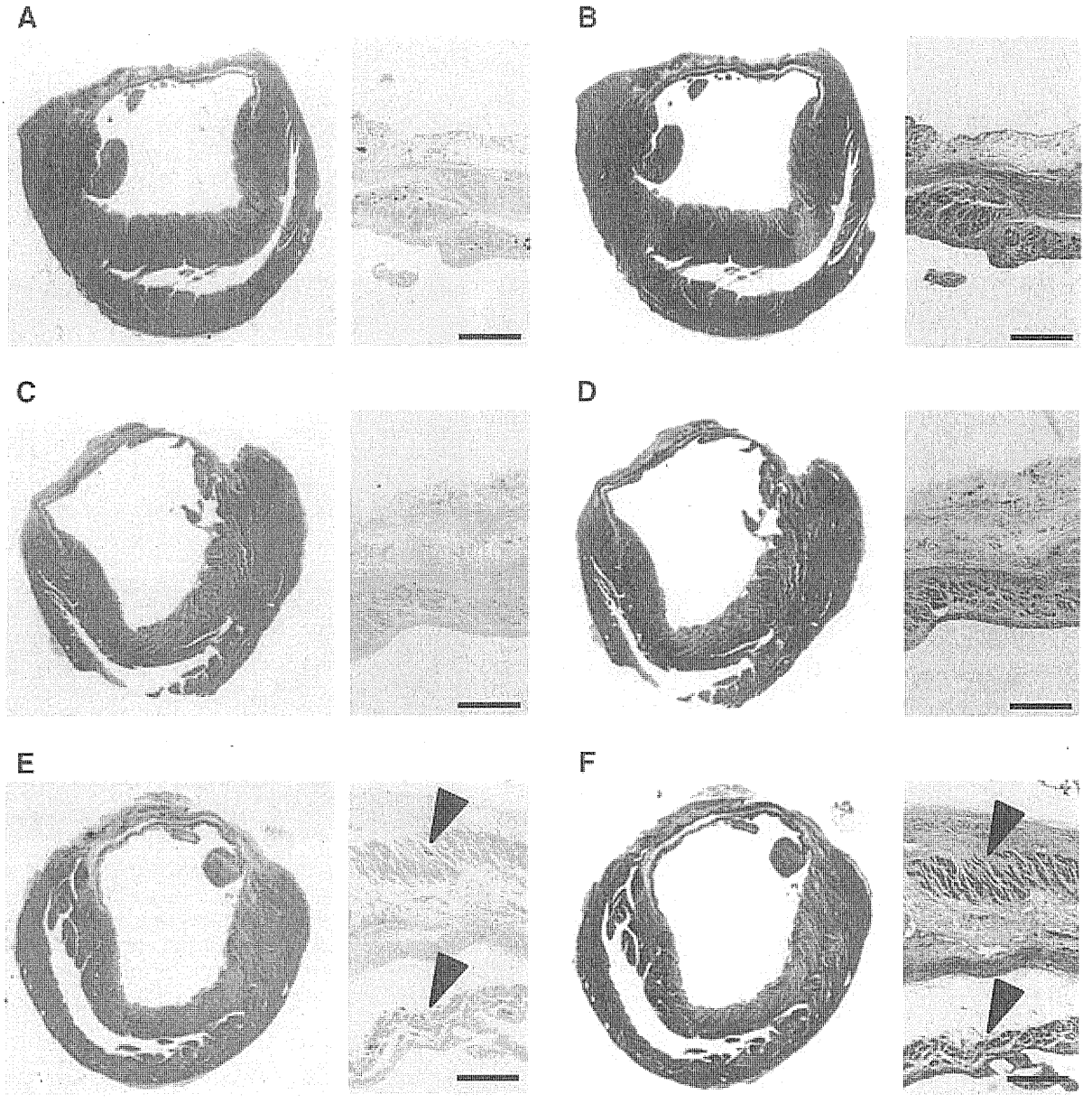

FIG. 3. Effects of CLC transplantation on cardiac structure. Photomicrographs showing representative myocardial sections stained with hematoxylin and eosin (A, C, D) and Masson trichrome (B, D, F) in the individual groups. The transplanted CLC patch reversed wall thinning of the infracted myocardium and another cardiac muscle was layered onto the transplanted area (arrowheads). (A, B) Sham-operated MI control group; (C, D) noncommitted hADMSC patch-transplanted group; and (E, F) hADMSC-derived CLC patch-transplanted group. Bars = 200 μm.

layer of α-CA-positive cells was apparent in the tissues from noncommitted hADMSC-transplanted rats (Fig. 4A, C), whereas the CLC patch-transplanted group showed two cardiac muscle layers positive for α-CA (Fig. 4E, arrow and arrowhead). There were no human troponin I-positive cells in the sham-operated MI control group (Fig. 4B), but some were observed in the noncommitted hADMSC patch-transplanted group (Fig. 4D). As shown in Figure 4F, large amounts of human troponin I-positive myocardium was observed in the CLC-transplanted animals (arrow) in addition to some human troponin I-negative but α-CA-positive myocardium in the internal myocardial layer (Fig. 4E, F, arrowhead). These results indicated that CLCs can efficiently differentiate into cardiomyocytes *in situ*.

Discussion

There are several advantages to hADMSC-derived CLC patch transplantation for regeneration therapy. First, the source of adipose-derived cells is easily and safely accessible and the cells can be obtained in large quantities, without serious ethical issues. Second, hADMSCs differentiate into CLCs by induction with DMSO, which is available in current good manufacturing practice grade. Third, hADMSC-derived

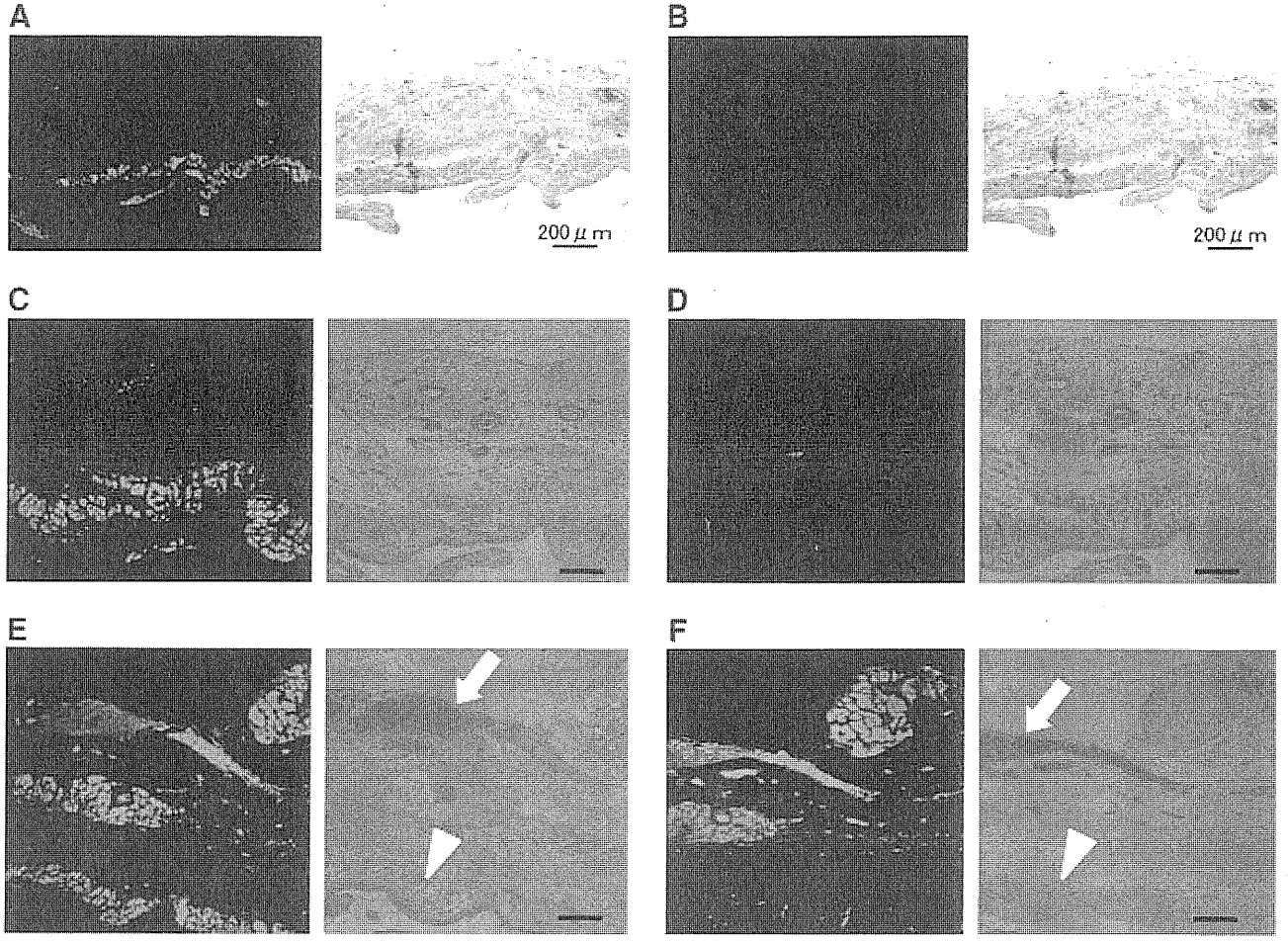

FIG. 4. CLCs differentiate into cardiac muscles *in situ*. Immunofluorescence with anti-α-CA (**A, C, E**) and anti-human-specific cardiac troponin I (**B, D, F**) antibodies, merged with phase contrast. In the hADMSC-derived CLC patch-transplanted groups, two cardiac muscle layers positive for α-CA are observed (**E**, arrow and arrowhead). A large mass of human troponin I-positive myocardium was observed in the CLC-transplanted tissues (**F**, arrows). In the same animals, the internal myocardium layer expressed α-CA but not human troponin I (**E, F**, arrowheads). (**A, B**) Sham-operated MI control group; (**C, D**) noncommitted hADMSC patch-transplanted group; and (**E, F**) CLC patch-transplanted group. Bars = 200 μm.

CLCs can differentiate into cardiomyocytes *in vivo* within the myocardial milieu, resulting in increment of myocardial muscle force. Finally, reconstruction of thick myocardial tissue rescued cardiac dysfunction after MI and improved long-term survival.

The choice of cell source is critical for realizing success in cellular therapy.[18] Liposuction surgeries yield from 100 mL to >3 L of lipoaspirate tissue.[19] The initial isolation of cells from adipose tissue was described by Bjorntorp *et al.*[14] This procedure was since modified to isolate cells from human adipose tissue specimens.[20–22] In this context, Zuk *et al.*[11] reported that the preadipocytes exhibited stem cell features as MSCs, currently known as ADMSCs. Because of the above-stated advantages of procuring cells for therapy from adipose tissues, hADMSCs present a potential and promising source for cellular therapy, even in patients with post-MI severe heart failure.

The *in vitro* differentiation of ADMSCs is now well reported, and experimental findings in recent years suggested considerable therapeutic potential for cellular replacement in the context of acute MI and chronic progressive cardiac disease.[23–27] Stem cells are differentiated into a cardiomyocyte lineage by treatment with 5-azacytidie, retinoic acid, oxytocin, and many other reagents.[28–32] We proposed that DMSO could differentiate hADMSCs into CLCs, based on the differentiation of P19 embryonic stems cells into cardiomyocytes with DMSO.[31–33] It was notable that DMSO is also available in current good manufacturing practice grade. Unfortunately, DMSO-treated hADMSCs did not show spontaneous beating as their terminal differentiation function, but the cells did express the mature markers α-*CA*, *myosin light chain*, and *myosin heavy chain* to a lesser extent. There are no reports of the use of DMSO to commit ADMSCs to a cardiomyocytic lineage. The mechanism by which DMSO elicits its effect on differentiation remains unclear. It is possible that DMSO increases intracellular calcium ion concentration, thereby elevating phosphatidylethanolamine levels in the cells and controlling the distribution of protein kinase C to commit the P19 stem cells.[33–36] These mechanisms should be investigated further in the near future.

The *in vitro* differentiation of ADMSCs has been well reported,[23–27] although only a few reports relate to the differentiation of these cells into cardiomyocytes *in vivo*. Recently,

Miyahara *et al.*[13] reported the use of monolayered ADMSCs for myocardial repair. In their study, rat ADMSCs were isolated and grown as intact monolayer sheets using temperature-responsive culture dishes. Placement of the ADMSC sheets onto a scarred myocardium in rats resulted in diminished scarring and enhanced cardiac structure and function. Histological analysis demonstrated that the engrafted ADMSC sheets grew to form a thickened layer over the infarcted muscle that included newly formed vessels and a few cardiomyocytes. In our study, hADMSC-derived CLCs differentiated into cardiomyocytes in a myocardial milieu, indicated by the immunohistological results in which transplanted cells expressed human troponin I *in vivo*. Newly developed myocardium might augment cardiac function, and thus hADMSC patch transplantation was performed as a control. Cardiac dysfunction was rescued in a short term, although the numbers of cardiomyocytes derived from transplanted cells were low. In this context, Gimble *et al.*[19] suggested that hADMSCs might secrete angiogenic factors and/or antiapoptotic factors.

Transplantation of the hADMSC-derived CLC regenerated the thick myocardial tissues, rescued cardiac dysfunction after MI, and improved long-term survival rate compared with the noncommitted hADMSCs and sham-operated MI controls. The existing literature suggests that ADMSCs can be engrafted and survive within an infarcted myocardial milieu, acquire phenotypic markers consistent with cardiomyocytic and vascular-related lineages, and have a positive impact on structural and functional endpoints.[19,23–27] These are desirable outcomes for cardiac function and survival. However, few reports have applied long-term observation of the transplanted animals. Our study therefore observed the three rat groups for 16 weeks after transplantation. Only CLC transplantation provided the desired outcome at the experimental endpoint. Despite these encouraging results, much progress is needed to realize the hope of cell therapies for myocardial damage. First, delivery of the cell sheets to patients should be optimized for each given disease. Second, the issue of vascularization should be considered in the infracted or affected tissues after transplantation, because many small CLC patches would be necessary for a clinical cure. Finally, the value and impact of CLC patch transplantation should be confirmed in large animal models before embarking on clinical applications.

In conclusion, we showed that the phenotype of hADMSCs could be changed to that of CLCs by induction with DMSO. These hADMSC-derived CLCs engrafted into a scarred myocardium and differentiated into cardiomyocytes. The CLC patch transplantation also resulted in recovery of cardiac function and improved survival rate. Thus, transplantation of hADMSC-derived CLC patches in heart patients might be a potentially effective therapeutic strategy for cardiac tissue regeneration in the near future.

Acknowledgments

This report was supported in part by a grant-in-aid for Yoshiki Sawa from the New Energy and Industrial Technology Development Organization of Japan and in part by a grant-in-aid for Akifumi Matsuyama from the Ministry of Education, Culture, Sports, Science, and Technology of Japan.

Disclosure Statement

No competing financial interests exist.

References

1. Miyagawa, S., Sawa, Y., Taketani, S., Kawaguchi, N., Nakamura, T., Matsuura, N., and Matsuda, H. Myocardial regeneration therapy for heart failure hepatocyte growth factor enhances the effect of cellular cardiomyoplasty. Circulation **105**, 2556, 2002.
2. Miyagawa, S., Matsumiya, G., Funatsu, T., Yoshitatsu, M., Sekiya, N., Fukui, S., Hoashi, T., Hori, M., Yoshikawa, H., Kanakura, Y., Ishikawa, J., Aozasa, K., Kawaguchi, N., Matsuura, N., Myoui, A., Matsuyama, A., Ezoe, S., Iida, H., Matsuda, H., and Sawa, Y. Combined autologous cellular cardiomyoplasty using skeletal myoblasts and bone marrow cells for human ischemic cardiomyopathy with left ventricular assist system implantation: report of a case. Surg Today **39**, 133, 2009.
3. Taylor, D.A. Cell-based myocardial repair: how should we proceed? Int J Cardiol **95**, S8, 2004.
4. Chachques, J.C., Acar, C., Herreros, J., Trainini, J.C., Prosper, F., D'Attellis, N., Fabiani, J.N., and Carpentier, A.F. Cellular cardiomyoplasty: clinical application. Ann Thorac Surg **77**, 1121, 2004.
5. Pallante, B.A., and Edelberg, J.M. Cell sources for cardiac regeneration—which cells and why. Am Heart Hosp J **4**, 95, 2006.
6. Chiu, R.C. MSC immune tolerance in cellular cardiomyoplasty. Semin Thorac Cardiovasc Surg **20**, 115, 2008.
7. Pittenger, M.F., Mackay, A.M., Beck, S.C., Jaiswal, R.K., Douglas, R., Mosca, J.D., Moorman, M.A., Simonetti, D.W., Craig, S., Marshak, D.R. Multilineage potential of adult human mesenchymal stem cells. Science **284**, 143, 1999.
8. Jiang, Y., Jahagirdar, B.N., Reinhardt, R.L., Schwartz, R.E., Keene, C.D., Ortiz-Gonzalez, X.R., Reyes, M., Lenrik, T., Lund, T., Blackstad, M., Du, J., Aldrich, S., Lisberg, A., Low, W.C., Largaespada, D.A., Vertaille, C.M. Pluripotency of mesenchymal stem cells derived from adult marrow. Nature **418**, 41, 2002.
9. Pittenger, M.F., and Martin, B.J. Mesenchymal stem cells and their potential as cardiac therapeutics. Circ Res **95**, 9, 2004.
10. Toma, C., Pittenger, M.F., Cahill, K.S., Byrne, B.J., and Kessler, P.D. Human mesenchymal stem cells differentiate to a cardiomyocyte phenotype in the adult murine heart. Circulation **105**, 93, 2002.
11. Zuk, P.A., Zhu, M., Mizuno, H., Huang, J., Futrell, J.W., Katz, A.J., Benhaim, P., Lorenz, H.P., and Hedrick, M.H. Multilineage cells from human adipose tissue: implications for cell-based therapies. Tissue Eng **7**, 211, 2001.
12. Katz, A.J., Tholpady, A., Tholpady, S.S., Shang, H., and Ogle, R.C. Cell surface and transcriptional characterization of human adipose-derived adherent stromal (hADAS) cells. Stem Cells **23**, 412, 2005.
13. Miyahara, Y., Nagaya, N., Kataoka, M., Yanagawa, B., Tanaka, K., Hao, H., Ishino, K., Ishida, H., Shimizu, T., Kangawa, K., Sano, S., Okano, T., Kitamura, S., and Mori, H. Monolayered mesenchymal stem cells repair scarred myocardium after myocardial infarction. Nat Med **12**, 459, 2006.
14. Bjorntorp, P., Karlsson, M., Pertoft, H., Pettersson, P., Sjostrom, L., and Smith, U. Isolation and characterization of cells from rat adipose tissue developing into adipocytes. J Lipid Res **19**, 316, 1978.

15. Memon, I.A., Sawa, Y., Fukushima, N., Matsumiya, G., Miyagawa, S., Taketani, S., Sakakida, S.K., Kondoh, H., Aleshin, A.N., Shimizu, T., Okano, T., and Matsuda, H. Combined autologous cellular cardiomyoplasty with skeletal myoblasts and bone marrow cells in canine hearts for ischemic cardiomyopathy. J Thorac Cardiovasc Surg **130**, 1333, 2005.
16. Miyagawa, S., Sawa, Y., Sakakida, S., Taketani, S., Kondoh, H., Memon, I.A., Imanishi, Y., Shimizu, T., Okano, T., and Matsuda, H. Tissue cardiomyoplasty using bioengineered contractile cardiomyocyte sheets to repair damaged myocardium: their integration with recipient myocardium. Transplantation **80**, 1586, 2005.
17. Hata, H., Matsumiya, G., Miyagawa, S., Kondoh, H., Kawaguchi, N., Matsuura, N., Shimizu, T., Okano, T., Matsuda, H., and Sawa, Y. Grafted skeletal myoblast sheets attenuate myocardial remodeling in pacing-induced canine heart failure model. J Thorac Cardiovasc Surg **132**, 918, 2006.
18. Murry, C.E., Reinecke, H., and Pabon, L.M. Regeneration gaps: observations on stem cells and cardiac repair. J Am Coll Cardiol **47**, 1777, 2006.
19. Gimble, J.M., Katz, A.J., and Bunnel, B.A. Adipose = derived stem cells for regenerative medicine. Circ Res **100**, 1249, 2007.
20. Deslex, S., Negrel, R., Vannier, C., Etienne, J., and Ailhaud, G. Differentiation of human adipocyte precursors in a chemically defined serum-free medium. Int J Obes **11**, 19, 1987.
21. Hauner, H., Entenmann, G., Wabitsch, M., Gaillard, D., Ailhaud, G., Negrel, R., and Pfeiffer, E.F. Promoting effect of glucocorticoids on the differentiation of human adipocyte precursor cells cultured in a chemically defined medium. J Clin Invest **84**, 1663, 1989.
22. Hauner, H., Wabitsch, M., and Pfeiffer, E.F. Differentiation of adipocyte precursor cells from obese and nonobese adult women and from different adipose tissue sites. Horm Metab Res Suppl **19**, 35, 1988.
23. Parker, A.M., and Katz, A.J. Adipose-derived stem cells for the regeneration of damaged tissues. Expert Opin Biol Ther **6**, 567, 2006.
24. Rangappa, S., Entwistle, J.W., Wechsler, A.S., and Kresh, J.Y. Cardiomyocyte-mediated contact programs human mesenchymal stem cells to express cardiogenic phenotype. J Thorac Cardiovasc Surg **126**, 124, 2003.
25. Gaustad, K.G., Boquest, A.C., Anderson, B.E., Gerdes, A.M., and Collas, P. Differentiation of human adipose tissue stem cells using extracts of rat cardiomyocytes. Biochem Biophys Res Commun **314**, 420, 2004.
26. Planat-Benard, V., Menard, C., Andre, M., Puceat, M., Perez, A., Garcia-Verdugo, J.M., Penicaud, L., and Casteilla, L. Spontaneous cardiomyocyte differentiation from adipose tissue stroma cells. Circ Res **94**, 223, 2004.
27. Strem, B.M., Zhu, M., Alfonso, Z., Daniels, E.J., Schreiber, R., Beygui, R., MacLellan, W.R., Hedrick, M.H., and Fraser, J.K. Expression of cardiomyocytic markers on adipose tissue-derived cells in a murine model of acute myocardial injury. Cytotherapy **7**, 282, 2005.
28. Balana, B., Nicoletti, C., Zahanich, I., Graf, E.M., Christ, T., Boxberger, S., and Ravens, U. 5-Azacytidine induces changes in electrophysiological properties of human mesenchymal stem cells. Cell Res **16**, 949, 2006.
29. Gassanov, N., Er, F., Zagidullin, N., Jankowski, M., Gutkowska, J., and Hoppe, U.C. Retinoid acid-induced effects on atrial and pacemaker cell differentiation and expression of cardiac ion channels. Differentiation **76**, 971, 2008.
30. Paquin, J., Danalache, B.A., Jankowski, M., McCann, S.M., and Gutkowska, J. Oxytocin induces differentiation of P19 embryonic stem cells to cardiomyocytes. Proc Natl Acad Sci USA **99**, 9550, 2002.
31. Fathi, F., Murasawa, S., Hasegawa, S., Asahara, T., Kermani, A.J., and Mowla, S.J. Cardiac differentiation of P19CL6 cells by oxytocin. Int J Cardiol **134**, 75, 2009.
32. Swijnenburg, R.J., van der Bogt, K.E., Sheikh, A.Y., Cao, F., and Wu, J.C. Clinical hurdles for the transplantation of cardiomyocytes derived from human embryonic stem cells: role of molecular imaging. Curr Opin Biotechnol **18**, 38, 2007.
33. Skerjanc, I.S. Cardiac and skeletal muscle development in P19 embryonal carcinoma cells. Trends Cardiovasc Med **9**, 139, 1999.
34. Xu, F.Y., Fandrich, R.R., Nemer, M., Kardami, E., and Hatch, G.M. The subcellular distribution of protein kinase C-alpha, -epsilon, and -zeta isoforms during cardiac cell differentiation. Arch Biochem Biophys **367**, 17, 1999.
35. Xu, F.Y., Kardami, E., Nemer, M., Choy, P.C., and Hatch, G.M. Elevation in phosphatidylethanolamine is an early but not essential event for cardiac cell differentiation. Exp Cell Res **256**, 358, 2000.
36. Monzen, K., Shiojima, I., Hiroi, Y., Kudoh, S., Oka, T., Takimoto, E., Hayashi, D., Hosoda, T., Habara-Ohkubo, A., Nakaoka, T., Fujita, T., Yazaki, Y., and Komuro, I. Bone morphogenetic proteins induce cardiomyocyte differentiation through the mitogen-activated protein kinase kinase kinase TAK1 and cardiac transcription factors Csx/Nkx-2.5 and GATA-4. Mol Cell Biol **19**, 7096, 1999.

Address correspondence to:
Akifumi Matsuyama, M.D., Ph.D.
Department of Somatic Stem Cell Therapy
Foundation for Biomedical Research and Innovation
1-5-4-305 Minatojima-minamimachi
Chuo-ku, Kobe 650-0047
Japan

E-mail: akifumi-matsuyama@umin.ac.jp

Received: June 1, 2009
Accepted: July 21, 2009
Online Publication Date: September 5, 2009

Layered implantation of myoblast sheets attenuates adverse cardiac remodeling of the infarcted heart

Naosumi Sekiya, MD,[a] Goro Matsumiya, MD, PhD,[a] Shigeru Miyagawa, MD, PhD,[a] Atsuhiro Saito, PhD,[a] Tatsuya Shimizu, MD, PhD,[b] Teruo Okano, PhD,[b] Naomasa Kawaguchi, PhD,[c] Nariaki Matsuura, MD, PhD,[c] and Yoshiki Sawa, MD, PhD[a]

Objective: We previously showed that autologous myoblast sheets constructed with tissue-engineering techniques improved the function of the impaired heart. In this study, we evaluated the effects of layered myoblast sheets to clarify whether increasing the number of sheets provides improvement of cardiac function.

Methods: Myoblast sheets were constructed in dishes that release confluent cells from the dish surface via temperature reduction. Sixty infarcted Lewis rats underwent implantation of myoblast sheets on the infarcted area. There were 4 groups (n = 15 in each group): S1: one layer, S3: three layers, S5: five layers, and a sham group. We examined cardiac function by echocardiography and catheterization, mRNA expression by real time reverse-transcriptase polymerase chain reaction, and histology.

Results: The ejection fraction and end-systolic pressure–volume relationship in the S5 and S3 groups were significantly improved. End-diastolic area was significantly reduced in the S5 group. The mRNAs for hepatocyte growth factor, vascular endothelial growth factor, and stromal cell–derived factor-1 were all up-regulated in dose-dependent fashion. On histologic examination, fibrosis was most decreased in S5, and vascular density was increased. Cellular hypertrophy was attenuated in both the S5 and S3 groups. Elastic fibers were massively up-regulated in the infarction and implanted sheets in the S5 and S3 groups, with expression of the elastin gene.

Conclusions: Implantation of three- and five-layered myoblast sheets yields favorable results, with better improvement of cardiac function, induction of angiogenesis, more elastic fibers, and less fibrosis. Thus, layered myoblast sheets, in optimal numbers, may attenuate adverse cardiac remodeling of the infarcted heart.

Myocardial regeneration therapy has been widely performed for myocardial infarction (MI). Cell transplantation using skeletal myoblasts has commonly been undertaken in animal models as well as in clinical trials.[1,2] Most myoblast transplantation studies for cardiac failure have supported the feasibility and safety of this method.[3-6] In these studies, the method of cell transplantation was direct myocardial injection with a fine needle. However, needle injection has some disadvantages, including loss of transplanted cells by leakage, poor survival of grafted cells, myocardial damage resulting from injury by the needle and subsequent acute inflammation,[7,8] and the potential to cause a lethal arrhythmia.[6] To overcome these disadvantages, we investigated the efficacy of a novel transplantation technique using cell sheets grown in temperature-responsive dishes.[9] Myoblast sheets, without scaffolding, were implanted to treat cardiac impairment in small and large experimental animal models, and greater improvement of cardiac function was observed as compared with that obtained by needle injection and control groups.[10-13]

However, the method of cell delivery in these studies had several limitations, including the implantation method (implanting two-layered myoblast sheets with collagen film to keep the sheets on the heart) and delivery of an optimal number of cells. It has been unclear whether delivery of more cells will be more effective in inducing cardiac regeneration. It has also not been clearly determined whether increasing the number of layers would yield better results. Shimizu and coworkers[14] reported that transplanted three-layered sheets of cardiomyocytes could be vascularized in subcutaneous tissue without necrosis, but that sheets with four or five layers have areas with disorganized vasculature and primary ischemia.

Our previous reports[10,11] showed that implantation of two-layered, autologous myoblast sheets improved cardiac function and prevented remodeling of the infarcted heart. In this study, we tested whether increasing the number of layered myoblast sheets would enhance functional recovery and attenuate adverse cardiac remodeling of the infarcted heart to estimate the optimal number of myoblast sheet layers for regeneration of host heart.

From the Department of Cardiovascular Surgery,[a] Osaka University Graduate School of Medicine, Osaka; the Institute of Advanced Biomedical Engineering and Science,[b] Tokyo Women's Medical University, Tokyo; and the Department of Molecular Pathology,[c] Osaka University Graduate School of Allied Health Science, Osaka, Japan.

This work was supported by the New Energy and Industrial Technology Development Organization in Japan.

Read at the Eighty-eighth Annual Meeting of The American Association for Thoracic Surgery, San Diego, Calif, May 10–14, 2008.

Received for publication May 15, 2008; revisions received Jan 7, 2009; accepted for publication Feb 2, 2009.

Address for reprints: Yoshiki Sawa, MD, PhD, 2-2 Yamada-oka, Suita, Osaka, 565-0871, Japan (E-mail: sawa@surg1.med.osaka-u.ac.jp).

J Thorac Cardiovasc Surg 2009;138:985-93

0022-5223/$36.00

doi:10.1016/j.jtcvs.2009.02.004

ET/BS

Abbreviations and Acronyms

HGF = hepatocyte growth factor
LV = left ventricular
LVEF = left ventricular ejection fraction
MI = myocardial infarction
RT-PCR = reverse-transcription polymerase chain reaction
SDF-1 = stromal-derived factor 1
VEGF = vascular endothelial growth factor

MATERIAL AND METHODS

Isolation of Myoblasts and Construction of Myoblast Sheets

Myoblasts were isolated from the skeletal muscle of the anterior tibialis from 3-week-old male Lewis rats. The rats were humanely killed, and their skeletal muscles were excised and washed with Hanks balanced salt solution (Gibco, Grand Island, NY) containing 1× penicillin–streptomycin–amphotericin B (PSA; Gibco). After the removal of as much fibrous tissue, tendons, and fat tissue as possible, the muscles were minced and enzymatically dissociated with collagenase type II (Gibco) (5 mg/mL) and trypsin–ethylenediaminetetraacetic acid (Gibco) for 30 minutes. The cells were collected by centrifugation (5 minutes at 280*g*), and the enzyme reaction was arrested by adding 20% fetal bovine serum (ICN Biomedicals, Aurora, Ohio), after which the cells were spun again. The supernatant was discarded and the cells were resuspended in culture medium composed of Dulbecco modified Eagle solution (Gibco) with 20% fetal bovine serum and 1% penicillin–streptomycin–amphotericin B. The initial plating was performed in noncoated 150-mm dishes (Iwaki, Tokyo, Japan) for 4 hours. Secondary plating was performed in noncoated dishes for 20 hours. After being pre-plated twice, the nonadherent cells were placed in collagen-coated 150-mm dishes (Iwaki) and incubated for 3 days, after which cell passaging was performed into five collagen-coated dishes. When the cells became approximately 70% confluent after 7 days' cultivation, they were dissociated from the dishes with trypsin–ethylenediaminetetraacetic acid and reincubated on 35-mm temperature-responsive culture dishes (UpCell; Cellseed, Tokyo, Japan) at 37°C, with cell number adjusted to 3.0×10^6 per dish. More than 70% of these cells were actin-positive and 40% to 50% were desmin-positive (Figure 1, *A* to *D*). After 24 hours, the dishes were incubated at 20°C for 30 minutes. During that time, the myoblast sheets detached spontaneously to generate free-floating, monolayer cell sheets. After detachment, the area of the sheets decreased to 1.00 ± 0.05 cm^2, whereas the thickness increased to 100 ± 10.0 μm (Figure 1, *E*).

Animals and Surgical Procedures

Eight-week old male Lewis rats were used (220–250 g; Seac Yoshitomi Ltd, Fukuoka, Japan). All experimental procedures and protocols used in this investigation were reviewed and approved by the institutional animal care and use committee and are in accordance with the National Institutes of Health Guide for the Care and Use of Laboratory Animals (NIH Publication No. 85-23, revised 1996). The rats were anesthetized with ketamine (90 mg/kg) and xylazine (10 mg/kg), and MI was induced by ligation of the left anterior descending coronary artery under mechanical ventilation, as previously described.[15] Two weeks after the ligation, baseline cardiac functions were measured, and the infarcted rats underwent implantation of myoblast sheets via rethoracotomy. The rats were randomly divided into 4 treatment groups: (1) S1 group (one-sheet implantation); (2) S3 group (three-sheet implantation; (3) S5 group (five-sheet implantation); and a sham group (sham surgery alone). The myoblast sheets were implanted directly over the scar area without sutures. After detachment from the temperature-responsive dish, each sheet was picked up individually and applied to the surface of the heart. So that the sheet could be spread, the folded areas were gently stroked with wet, round tip forceps. After 3 to 5 minutes, subsequent sheets were applied by the same technique. After treatment, the pericardium was overwrapped by suturing with 8–0 Prolene polypropylene suture (Ethicon, Inc, Somerville, NJ) to prevent sheets from adhering to the chest wall.

Assessment of Cardiac Function

Left ventricular (LV) function of the treated rats was monitored by echocardiography 4 and 8 weeks after myoblast sheet implantation and compared with results before implantation (baseline). Cardiac ultrasonography was performed with a SONOS 5500 sonograph (Agilent Technologies, Palo Alto, Calif) using a 12-MHz annular array transducer under anesthesia with diethyl ether. The hearts were imaged in short-axis 2-dimensional views at the level of the papillary muscles, and LV end-systolic area, LV end-diastolic area, and the LV dimensions at end-systole and end-diastole (LVDs, LVDd) were determined. Fractional shortening was determined as ([LVDd − LVDs]/LVDd) × 100. Ejection fraction (EF) was calculated by the Pombo method, as $EF\ (\%) = ([LVDd^3 - LVDs^3]/LVDd^3) \times 100$.

Eight weeks after implantation, the rats were anesthetized and placed in a supine position on a controlled heating pad, and core temperature, measured via a rectal probe, was maintained at 37°C ± 1°C. A MicroTip catheter transducer (SPR-671; Millar Instruments, Inc, Houston, Tex) and conductance (Unique Medical Co, Tokyo, Japan) catheters were placed longitudinally in the left ventricle from the apex. We connected the catheters to an Integral 3 signal conditioner–processor (Unique Medical Co, Tokyo, Japan). LV pressure and volume and the electrocardiogram were displayed and digitized on a personal computer. LV pressure–volume relations were measured by transiently compressing the inferior vena cava. Data were recorded as a series of pressure–volume loops (about 20 loops). The pressure–volume loop data were analyzed with Integral 3 software (Unique Medical Co).[16]

Histologic Examination

LV myocardial specimens were obtained 4 weeks after sheet implantation. Each specimen was fixed with 10% buffered formalin and embedded in paraffin. Hematoxylin and eosin and Masson's elastica staining were performed. Picrosirius red staining to detect myocardial fibrosis and periodic acid–Schiff staining for cardiomyocyte hypertrophy were performed for specific treatment groups, as described.[17] Anterior wall thickness was measured in at least 3 hematoxylin and eosin–stained sections of the middle portion of the left ventricle of each heart. To label vascular endothelial cells, so that blood vessels could be counted, we performed immunohistochemical staining for factor VIII–related antigen according to a modified protocol. We used EPOS-conjugated antibody to factor VIII–related antigen coupled with HRP (Dako EPOS Anti-human von Willebrand Factor/HRP; Dako, Carpenteria, Calif) as primary antibody. The stained vascular endothelial cells were counted under a light microscope. Results were expressed as the number of blood vessels per square millimeter. Quantitative morphorometric analysis for each sample was performed with MacScope software (Mitani Corporation, Tokyo, Japan). Myocardial fibrosis was expressed as percent fibrosis, the fraction of red-stained area in total myocardium, with results obtained from 10 fields per section per animal. To determine myocyte cell size, we randomly selected 10 fields from each ventricle and measured 5 randomly chosen myocytes per field.

Measurement of Growth Factors and Elastin Gene Expression After Implantation

Infarcted and noninfarcted LV myocardium from the rats having a ligated left anterior descending coronary artery was removed 4 weeks

ET/BS

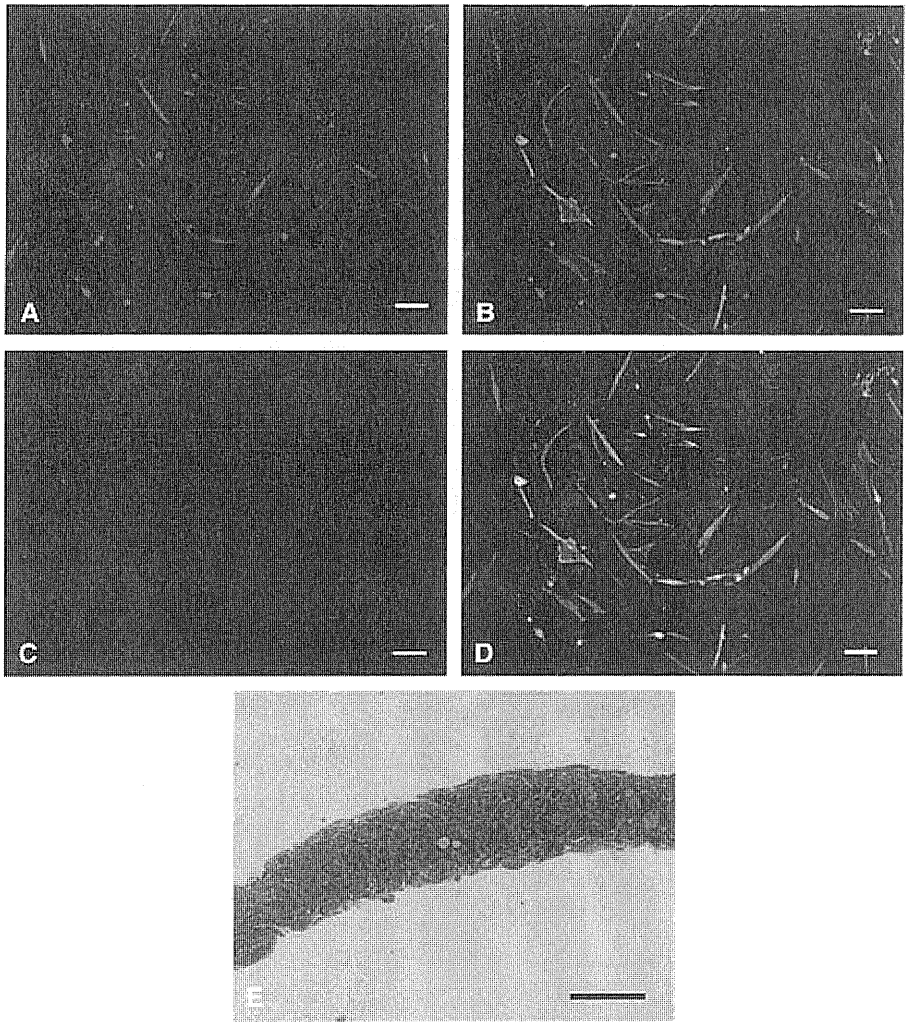

FIGURE 1. Cultured myoblasts and cross section of a sheet. Almost all cultured cells were actin-positive (A), and roughly 40% to 50% of them were desmin-positive muscle lineage cells (B). DAPI (4,6-diamino-2-phenylindole) staining of nuclei (C), and merged image (D) (A–D; magnification ×10, *bar* = 100 μm). Toluidine blue staining of cross section of sheet-constructed cells (E) (*bar* = 100 μm).

after implantation and immediately stored in RNA*later* solution (Qiagen, Hilden, Germany) until use (n = 10 for each of the 4 groups, S1, S3, S5, and sham). Total RNA was extracted with the RNeasy mini kit (Qiagen), and relative levels of mRNA transcripts were measured by the real-time quantitative reverse-transcriptase polymerase chain reaction (RT-PCR) technique using the ABI PRISM 7700 Sequence Detection System (Applied biosystems, Carlsbad, Calif).[18] The average copy number of gene transcripts in each sample was normalized to that for glyceraldehyde-3-phosphate dehydrogenase, and fold induction of each gene was calculated by the formula: Fold induction = Normalized value in a sample after MI/Mean of the normalized values for 15 reference myocardial samples.

Data Analyses

All values are the mean ± standard error of the mean. To assess the significance of differences between individual groups, we performed statistical evaluations with multiple analyses of variance. Differences in cardiac function data obtained by echocardiography were assessed by 2-way repeated-measures analysis of variance. If a significant F ratio was obtained, further analysis was carried out with a post hoc test.

RESULTS

Layered Myoblast Sheet Implantation Improved Cardiac Performance

Echocardiography revealed significant improvement of LV ejection fraction (LVEF) and percentage fractional shortening in the S3 and S5 groups compared with the S1 and sham groups 4 and 8 weeks after implantation. The LVEF 4 weeks after implantation in the S5 group was significantly improved compared with that in the S3 group ($P < .05$) (Figure 2, *A* and *B*). Enlargement of LV end-diastolic area was significantly attenuated in the S5 group compared with the sham and S1 groups at 4 weeks and differed significantly from the sham group 8 weeks after implantation (Figure 2, *C*). The end-systolic pressure–volume relationship was significantly improved in both the S3 and S5 groups compared with the S1 and sham groups 8 weeks after implantation (Figure 2, *D*). Thus, implantation of sheets of at

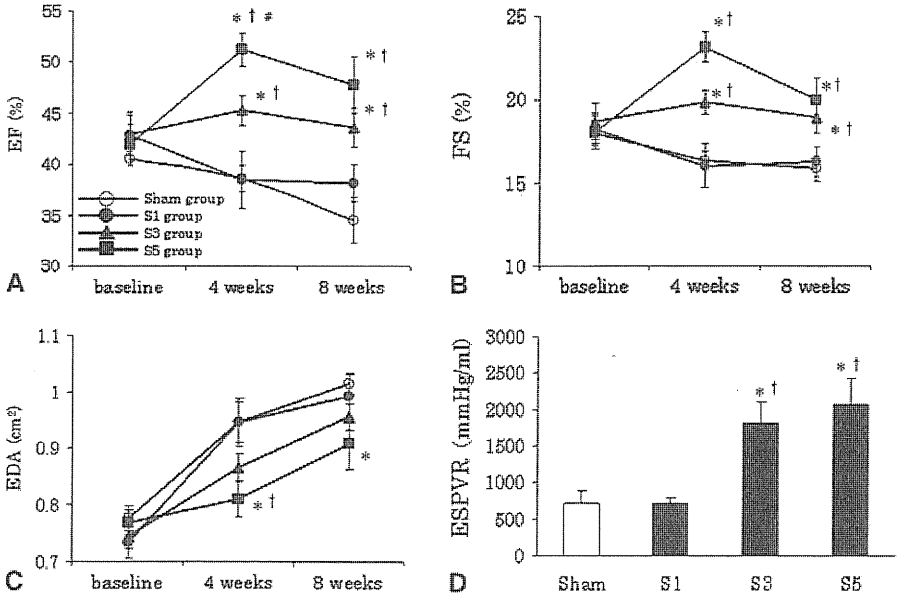

FIGURE 2. Cardiac function after layered myoblast sheet implantation. Echocardiographic measurements of rat heart (A–C). *Baseline* represents 2 weeks after left anterior descending coronary artery ligation. The pressure-volume study was performed at 8 weeks after treatment to estimate the systolic function of rat heart (D). *$P < .05$ versus sham group. †$P < .05$ versus S1 group. #$P < .05$ versus S3 group. *EF*, Ejection fraction; *FS*, fractional shortening; *EDA*, end-diastolic area; *ESPVR*, end-systolic pressure-volume relationship.

least three layers improved systolic function of the impaired heart, although only implantation of five-layered sheets attenuated enlargement of the left ventricle after infarction.

Histologic Improvement of Host Heart After Myoblast Sheet Implantation

Anterior wall thickness increased in a dose-dependent fashion. Three- and five-sheet implantations significantly thickened the infarcted wall compared with other conditions ($P < .05$) (Figure 3, *A* to *D*, and Figure 4, *A*). In the infarcted region 4 weeks after implantation, vascular density was significantly higher in the S3 and S5 groups than in the S1 and sham groups ($P < .05$). There was no significant difference in density between the S3 and S5 groups (Figure 3, *E* to *H*, and Figure 4, *B*). In noninfarcted regions at 4 weeks, picrosirius red staining revealed significant reduction of fibrosis in the S3 and S5 groups compared with the S1 and sham groups. The fibrosis in the S5 group was significantly reduced compared with that in the S3 group (Figure 3, *I* to *L*, and Figure 4, *C*). The mean diameters of the myocytes in the S3 and S5 groups were smaller than those in the S1 and sham groups ($P < .05$) (Figure 3, *M* to *P*, and Figure 4, *D*).

Assessment of Growth Factors by Gene Expression

RT-PCR analysis 4 weeks after implantation revealed significantly higher expression of stromal-derived factor 1 (SDF-1) in the S5 group than in the other groups ($P < .05$). Although expression of vascular endothelial growth factor (VEGF) increased in each group in a dose-dependent fashion, there were no significant differences among groups. The hepatocyte growth factor (HGF) gene was expressed to significantly higher levels in the S1, S3, and S5 groups than in the sham group (Figure 5). Thus, the hearts implanted with myoblast sheets expressed angiogenetic factors in a dose-dependent fashion, and increasing the number of myoblast sheets yielded greater expression of growth factors.

Increase in Elastic Fibers in Implanted Area With Expression of Tropoelastin mRNA

Masson's elastica staining showed that elastic fibers had increased not only in the implanted sheet layers but also in the infarcted scar area. In the S5 and S3 groups, the implanted sheets including elastic fibers surrounded the host heart over the infarcted area (Figure 6, *A* to *D*). In contrast, they were scarce in the S1 and sham groups (Figure 6, *E* and *F*). The relative expression of rat tropoelastin mRNA increased in a dose-dependent fashion. Expression in the S5 group was significantly higher than those in the sham and S1 groups ($P < .05$) (Figure 6, *G*).

DISCUSSION

In this study, we examined whether increasing the number of cell sheets used to attenuate cardiac remodeling and repair an infarcted myocardial wall improved cardiac performance. We found that implantation of five-layered myoblast sheets yielded favorable results, with improvement of cardiac function, induction of angiogenesis, less fibrosis, and less hypertrophy than the single-layered sheets used in this study or the two-layered sheets used in previous studies.[10,11] Sheet-shaped tissue maintains intact membrane and adhesive

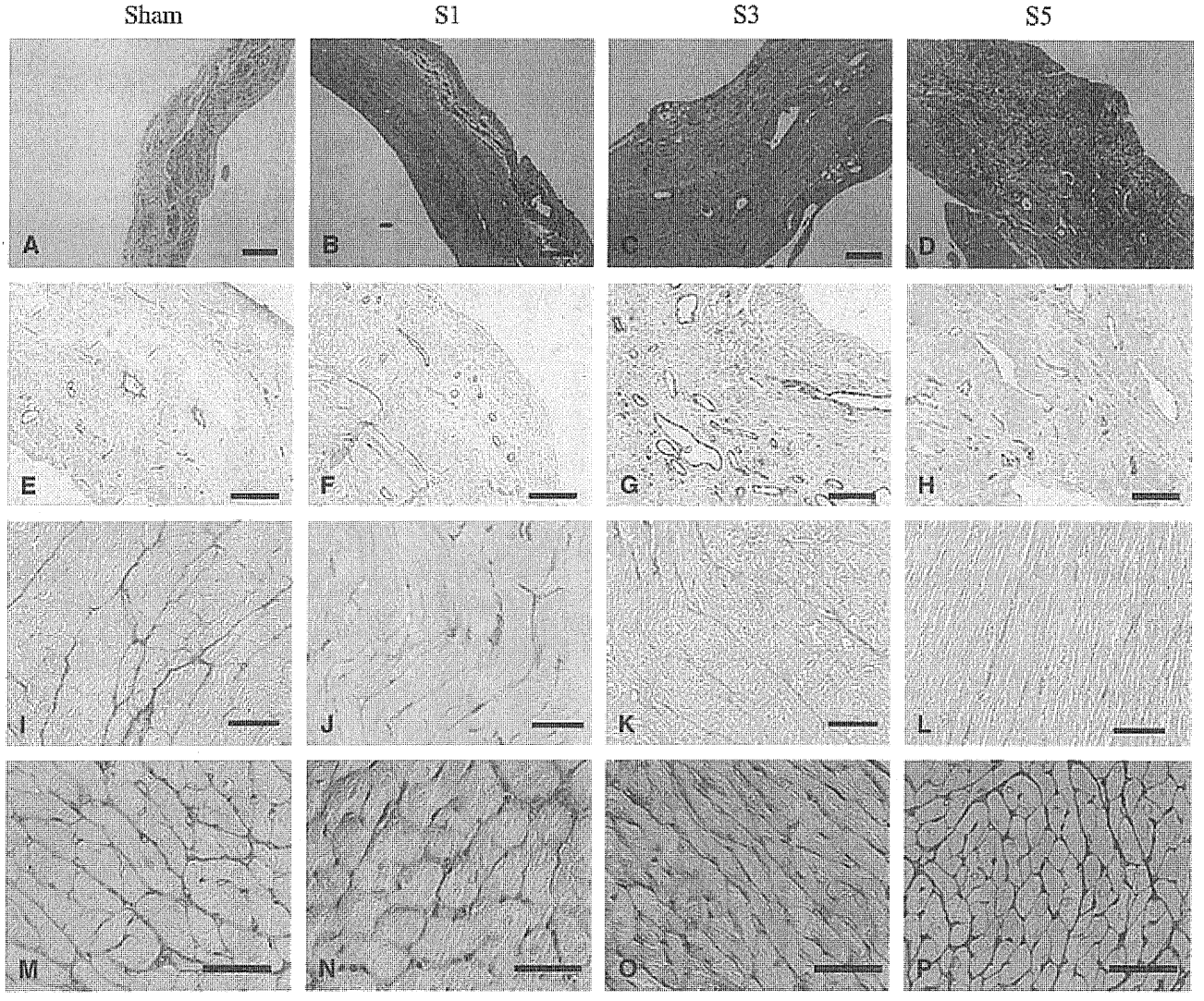

FIGURE 3. Histologic findings of implanted host hearts. Macroscopic (×20) view of anterior wall of hearts (hematoxylin and eosin stain): sham, A; S1, B; S3, C; S5, D (*bar* = 200 μm). Sections of infarcted regions were stained with antibody to von Willebrand factor (factor VIII): sham, E; S1 F; S3, G; S5, H (*bar* = 100 μm). Sirius-red staining of myocardium of noninfarcted regions: sham, I; S1, J; S3, K; S5, L (*bar* = 100 μm). Periodic acid–Schiff–stained myocardium of noninfarcted regions: sham, M; S1, N; S3, O; S5, P (*bar* = 50 μm).

proteins, incorporates extracellular matrix molecules, secretes growth factors owing to favorable cell-to-cell crosstalk, and prevents cellular microenvironment disruption by enzymatic reactions typically used to detach cells from tissue culture dishes (eg, trypsin or dispase).[19] These new tissue-engineered cell sheets are expected to be useful for cell delivery to the heart.[6,1,12]

Cardiac remodeling after MI appears to be compensatory initially, but has generally adverse effects and is linked to the progression of heart failure. Cardiomyocyte hypertrophy and interstitial fibrosis are usually observed in the remodeled heart, and greater ventricular enlargement correlates with a poorer prognosis for patients with coronary artery disease.[20,21] It is, therefore, now widely believed that ventricular remodeling is an important therapeutic target in patients with MI. Here, we treated MI hearts by implantation of layered myoblast sheets and observed decreased remodeling. The mechanism of this attenuation of remodeling may involve efficient delivery of myoblast sheets that overlap the scar area and its borders in the form of a cellular bridge.[11]

Expression of HGF, VEGF, and SDF-1 increases in the host heart implanted with myoblast sheets.[11] Therefore, layered myoblast sheets may be good suppliers of these factors for impaired hearts. HGF prevents the ventricular remodeling of hearts with established experimental MI.[22-25] Our previous findings suggested that SDF-1 is released from myoblasts, recruits hematopoietic stem cells, and facilitates repair of the infarcted heart. Similarly, the increased release of HGF and VEGF in the S3 and S5 treatment groups of the current study might have had advantageous effects in

ET/BS

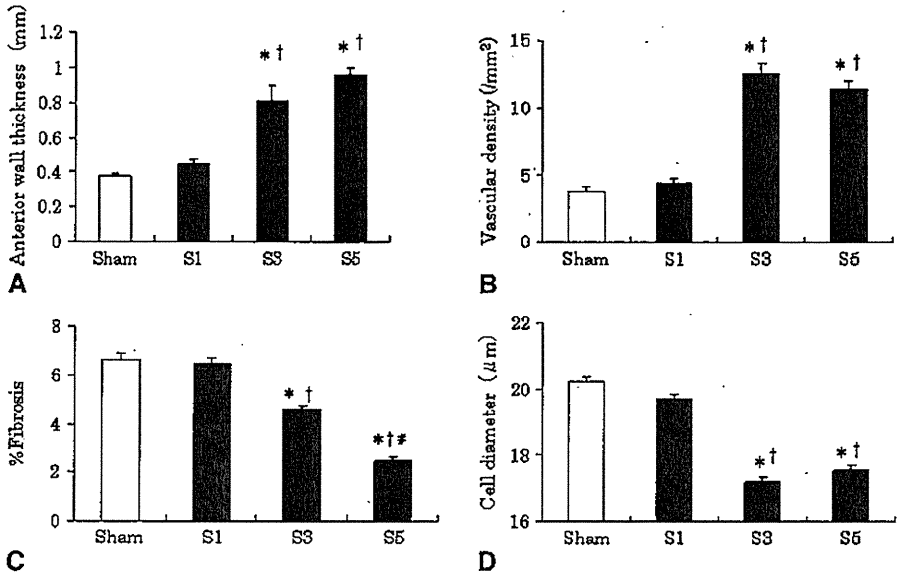

FIGURE 4. Quantitative assessment of histologic findings. A, Assessment of anterior wall thickness after implantation. B, Assessment of vascular density in the infarcted area of host hearts vascular density. C, Quantitative results for fibrotic change in the left ventricle. D, Cardiomyocyte short-axis diameters were measured as described in Methods (n = 5 for each group: A–D, 10 randomly chosen fields per section: B–D). *$P < .05$ versus sham group. †$P < .05$ versus S1 group. #$P <$. 05 versus S3 group.

the damaged heart. On histologic examination, microvessels were increased in the infarcted areas implanted with myoblast sheets. This increased angiogenesis, likely caused by increased HGF, VEGF, and SDF-1, may have improved the microenvironment of the myocytes, rescuing them from cell death or scar formation.

Elastin is a major insoluble extracellular matrix component. The elastic fiber network provides tissue with the critical properties of elasticity and resilient recoil and maintains the integrity of tissue architecture against repeated expansion.[26,27] Mizuno and colleagues[28] reported that transplantation of elastin gene–transfected cells attenuated adverse

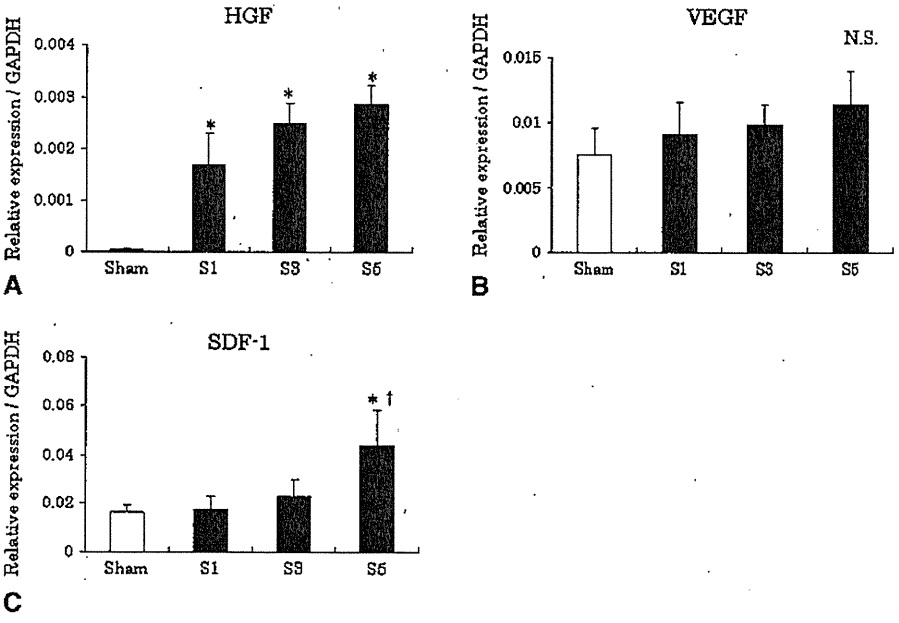

FIGURE 5. Relative expression of growth factors (A–C). Relative levels of mRNA transcripts were measured by the real-time quantitative RT-PCR (n = 10 for each of the four groups, S1, S3, S5, and sham). The average copy number of gene transcripts in each sample was normalized to that for glyceraldehyde-3-phosphate dehydrogenase *(GAPDH)*. *$P < .05$ versus sham group. †$P < .05$ versus S1 group. *HGF*, Hepatocyte growth factor; *VEGF*, vascular endothelial growth factor; *SDF-1*, stromal-derived factor-1.

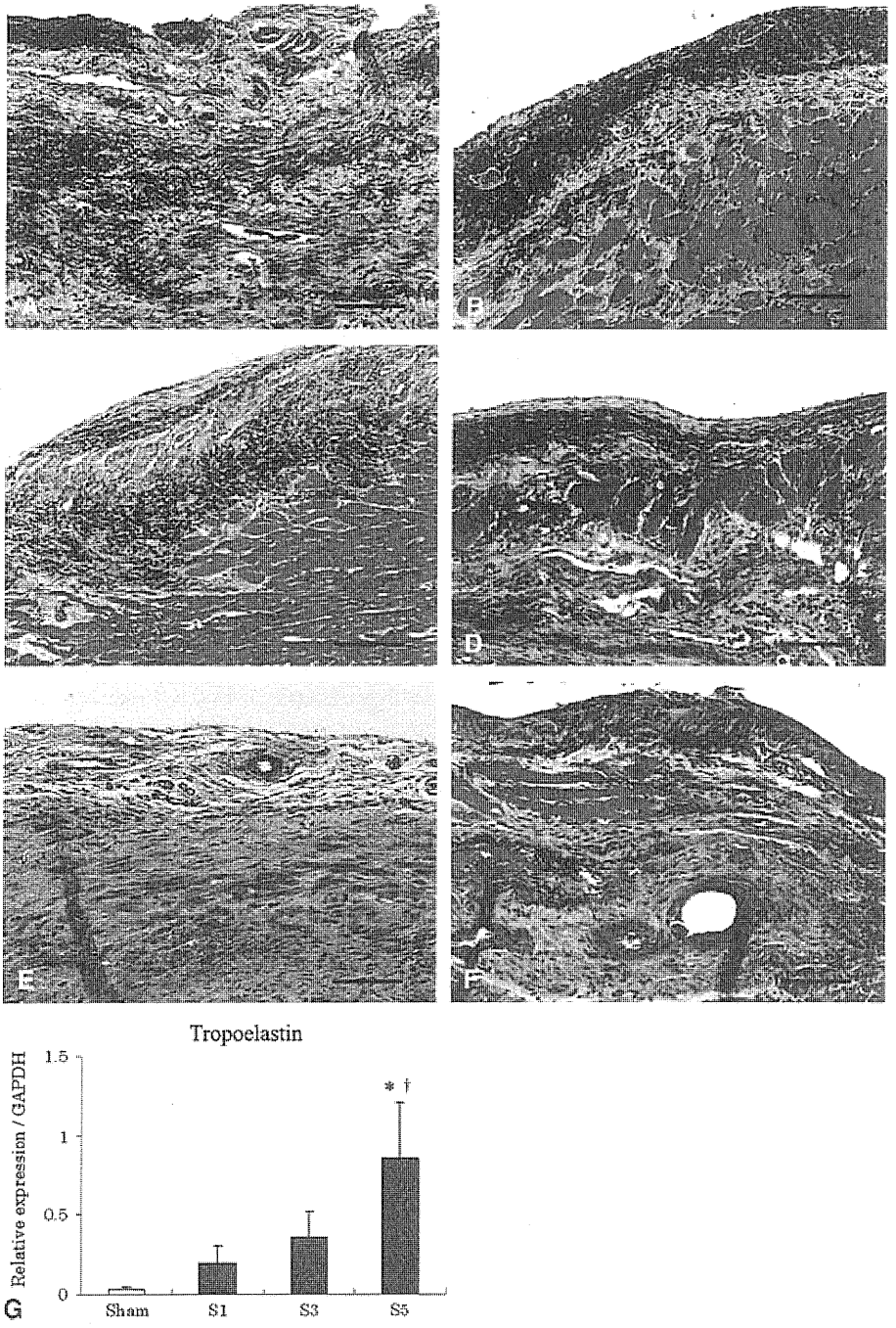

FIGURE 6. Elastic fibers were constructed after implantation, with expression of mRNA. Elastic fibers were increased in sheets and host infarcted area in the S5 and S3 groups (S5, A and B; S3, C and D). There were few elastic fibers in the S1 and sham groups (S1, E; sham, F). Relative expression of mRNA of tropoelastin (G). *$P < .05$ versus sham group. †$P < .05$ versus S1 group.

cardiac remodeling of the infarcted heart. The underlying mechanism may involve the addition of elasticity to the infarcted area, permitting recoil in response to the stresses of contraction, which might reduce scar thinning and dilatation. In our studies, implanted myoblast sheets organized elastic fibers not only in the sheet cells but also in the infarcted area of the host heart. Layered myoblast sheet cells might organize the elastic fibers within the cell sheets and infarcted area via expression of tropoelastin, which was expressed more strongly in the layered implantation groups (S3 and S5). It may thus provide elasticity to the host heart, with the improvement of systolic function and less LV dilatation.

We have never detected procedure-induced arrhythmia in these animal models.[11-13] Menasché and associates[6] reported

ET/BS

that sustained ventricular tachycardia might be an adverse effect after myoblast injection. The implantation of myoblast sheets seems to be safe in this regard. We speculate that myoblasts implanted into the heart may have the potential to cause random electrical activity, causing lethal arrhythmia. On the other hand, myoblast sheets implanted outside the epicardium may not generate sufficient aberrant electrical activity to cause lethal arrhythmia. Of course, this is speculation and further investigation, including electrophysiologic studies, is needed.

One of the limitations of this study is that implantation of more than five layers of myoblast sheets was not investigated. However, we tested ten-layered–sheet implantation in this model and found that the LVEF in this group improved to the same level as seen in the S5 group 4 and 8 weeks after implantation (Sekiya and Sawa; unpublished results). This suggests that improvement of cardiac function may plateau at five layers because of the insufficient supply of oxygen and nutrition for myoblasts. This contrasts with the study of Shimizu and associates,[14] who found that a maximum of three layers could be implanted at one time using cardiomyocyte sheets. Therefore, myoblasts may have a higher tolerance against ischemia and/or hypoxia than cardiomyocytes, and five-layered sheets could be more optimal than three-layered sheets when myoblast sheets are implanted.

Another limitation is of the current study is that the fate of the implanted cells was not tracked. We have begun addressing this by examining sheet cell survival 4 weeks after implantation. In brief, we transplanted male-derived cell sheets onto 15 female infarct hearts that were divided into three groups (S1, one sheet; S3, three sheets; S5, five sheets; $n = 5$ in each group). Four weeks later, genomic DNA was purified from the whole heart, and the male-specific SRY gene, which represented the implanted cells and their derivatives, was measured by real-time quantitative PCR.[29] The expression ratio of SRY to interleukin 2 gene was as follows (%): S1 (0.05 ± 0.01) < S3 (0.22 ± 0.10, $P < .05$ vs S1) < S5 (0.86 ± 0.16, $P < .05$ vs S1, S3) ($n = 5$, each group) (Sekiya and Sawa; unpublished results). From these results, we found that more cells survived on the host heart 4 weeks after implantation when a greater number of sheets were implanted. This fact could not directly assess the sheet cell survival on male donor rats. However, we believe that layered sheet implantation yields dose-dependent cell survival after implantation. Although we do not yet know the phenotype of these implanted cells, the survival data were compatible with the dose-dependent growth factor expression and increased wall thickness seen in the experiments presented here.

We propose the following mechanism of repair of the infarcted heart by layered myoblast sheets. At first, the implanted sheets might provide angiogenic and cardioprotective factors, such as HGF, VEGF, and SDF-1, to the host heart. These factors induce angiogenesis in the infarcted area. Additionally, the myoblast sheets mechanically cover the infarcted area and increase its thickness. Then, the implanted sheet cells express the elastin gene and form elastic fibers both in the sheets and in the host heart. The repaired heart, in turn, exhibits reduced wall stress, and LV dilatation, fibrosis, and hypertrophy are prevented.

Recently, we[30] have investigated 3-dimensional cell sheet construction in vitro using combinations of several different kinds of cells, such as endothelial cells and fibroblasts, aiming to induce vasculogenesis in cell sheets. In the future, beating cell sheets differentiated from pleuripotent stem cells, expressing connexin 43, and containing endothelial cells might be applied to the impaired heart and yield even greater improvement of cardiac function via different mechanisms, such as direct mechanical support through gap junctions, than those reported here.

In summary, our study demonstrated that implantation of myoblast sheets with five layers significantly improved LV systolic function for at least 2 months. Although the mechanism of this effect is not yet clear, a paracrine activity might induce angiogenesis and reduce fibrosis and hypertrophy. Elastic fibers in the cell sheets or host heart might mechanically improve the function of the infarcted heart. Thus, layered myoblast sheets, in optimal numbers, may improve cardiac function and attenuate adverse cardiac remodeling in the infarcted heart. A clinical trial is desired in the near future.

We thank Mrs Masako Yokoyama and Mr Kazuhiro Takekita for their excellent technical assistance and Dr Shannon L. Wyszomierski for correcting the grammar in the manuscript.

References

1. Taylor DA, Atkins BZ, Hungspreugs P, Jone TR, Reedy MC, Hutcheson KA, et al. Regenerating functional myocardium: improved performance after skeletal myoblast transplantation. *Nat Med.* 1998;4:929-33.
2. Chachques JC, Acar C, Herreros J, Trainini JC, Prosper F, D'Attellis N, et al. Cellular cardiomyoplasty: clinical application. *Ann Thorac Surg.* 2004;77:1121-3.
3. Menasché P, Hagege AA, Scorsin M, Puzet B, Desnos B, Schwartz K, et al. Myoblast transplantation in heart failure. *Lancet.* 2001;357:279-80.
4. Hagege AA, Marolleau JP, Vilquin JT, Alheritiere A, Peyrard S, Duboc D, et al. Skeletal myoblast transplantation in ischemic heart failure: long-term follow-up of the first phase I cohort of patients. *Circulation.* 2006;114:I108-13.
5. Dib N, Michler RE, Pagani FD, Wright S, Kereiakes DJ, Lengerich R, et al. Safety and feasibility of autologous myoblast transplantation in patients with ischemic cardiomyopathy: four-year follow-up. *Circulation.* 2005;112:1748-55.
6. Menasché P, Hagege AA, Vilquin JT, Desnos M, Abergel E, Pouzet B, et al. Autologous skeletal myoblast transplantation for severe postinfarction left ventricular dysfunction. *J Am Coll Cardiol.* 2003;41:1078-83.
7. Pagani FD, DerSimonian H, Zawadzka A, Wetzel K, Edge AS, Jacoby DB, et al. Autologous skeletal myoblasts transplanted to ischemia-damaged myocardium in humans. Histological analysis of cell survival and differentiation. *J Am Coll Cardiol.* 2003;41:1078-83.
8. Suzuki K, Murtuza B, Fukushima S, Smolenski RT, Varela-Carver A, Coppen SR, et al. Targeted cell delivery into infarcted rat hearts by retrograde intracoronary infusion: distribution, dynamics, and influence on cardiac function. *Circulation.* 2004;110(Suppl II):II-225-30.
9. Okano T, Yamada N, Okuhara M, Sakai H, Sakurai Y. Mechanism of cell detachment from temperature-modulated, hydrophilic-hydrophobic polymer surfaces. *Biomaterials.* 1995;16:297-303.
10. Miyagawa S, Sawa Y, Kitagawa-Sakakida S, Taketani S, Kondoh H, Memon IA, et al. Tissue cardiomyoplasty using bioengineered contractile cardiomyocyte sheets to repair damaged myocardium: their integration with recipient myocardium. *Transplantation.* 2005;80:1586-95.

ET/BS

11. Memon IA, Sawa Y, Fukushima N, Matsumiya G, Miyagawa S, Taketani S, et al. Repair of impaired myocardium by means of implantation of engineered autologous myoblasts sheets. *J Thorac Cardiovasc Surg.* 2005;130:1333-41.
12. Kondoh H, Sawa Y, Miyagawa S, Sakakida-Kitagawa S, Memon IA, Kawaguchi N, et al. Longer preservation of cardiac performance by sheet-shaped myoblast implantation in dilated cardiomyopathy hamsters. *Cardiovasc Res.* 2005;69:466-75.
13. Hata H, Matsumiya G, Miyagawa S, Kondoh H, Kawaguchi N, Matsuura N, et al. Grafted skeletal myoblast sheets attenuate myocardial remodeling in pacing-induced canine heart failure model. *J Thorac Cardiovasc Surg.* 2006;132: 918-24.
14. Shimizu T, Sekine H, Yang J, Isoi Y, Yamato M, Kikuchi A, et al. Polysurgery of cell sheet grafts overcomes diffusion limits to produce thick, vascularized myocardial tissues. *FASEB J.* 2006;20:708-10.
15. Wiesman HF, Bush DE, Mannisi JA, Weisfeldt ML, Healy B. Cellular mechanism of myocardial infarct expansion. *Circulation.* 1988;78:186-201.
16. Nishio R, Sasayama S, Matsumori A. Left ventricular pressure–volume relationship in a murine model of congestive heart failure due to acute viral myocarditis. *J Am Coll Cardiol.* 2002;40:1506-14.
17. Lekgave ED, Kiriazis H, Zhao C, Xu Q, Moore XL, Su Y, et al. Relaxin reverses cardiac and renal fibrosis in spontaneously hypertensive rats. *Hypertension.* 2005; 46:412-8.
18. Horiguchi K, Sakakida-Kitagawa S, Sawa Y, Li ZZ, Fukushima N, Shirakura R, et al. Selective chemokine and receptor gene expressions in allografts that develop transplant vasculopathy. *J Heart Lung Trasnplant.* 2002;21: 1090-100.
19. Kushida A, Yamato M, Okano T, Kikuchi A, Sakurai Y, Okano T. Decrease in culture temperature releases monolayer endothelial cell sheets together with deposited fibronectin matrix from temperature-responsive culture surfaces. *J Biomed Mater Res.* 1999;45:355-62.
20. Sharpe N. Cardiac remodeling in coronary artery disease. *Am J Cardiol.* 2003; 93(suppl):17B-20B.
21. Opie LH, Commerford PJ, Gersh BJ, Pfeffer MA. Controversies in ventricular remodeling. *Lancet.* 2006;367:356-67.
22. Cittandini A, Grossman BA, Raffaele N, Katz S, Stromer H, Smith RJ, et al. Growth hormone attenuates early left ventricular remodeling and improves cardiac function in rats with large myocardial infarction. *J Am Coll Cardiol.* 1997;29:1109-16.
23. Li Y, Takemura G, Kosai K, Yuge K, Nagano S, Esaki M, et al. Postinfarction treatment with an adenoviral vector expressing hepatocyte growth factor relieves chronic left ventricular remodeling and dysfunction in mice. *Circulation.* 2003;107:2499-506.
24. Askari AT, Unzek S, Popovic ZB, Goldman CK, Torudi F, Penn MS, et al. Effect of stromal-cell–derived factor 1 on stem-cell homing and tissue regeneration in ischemic cardiomyopathy. *Lancet.* 2003;362:697-703.
25. Rarajczak MZ, Majaka M, Kucia M, Drukala J, Piper S, Janowska WA, et al. Expression of functional CXCR4 by muscle satellite cells and secretion of SDF-1 by muscle-derived fibroblasts is associated with the presence of both muscle progenitors in bone marrow and hematopoietic stem/progenitor cells in muscles. *Stem Cell.* 2003;21:363-71.
26. Kielty CM, Sherratt MJ, Shuttleworth CA. Elastic fibers. *J Cell Sci.* 2002;115: 2817-28.
27. Nakamura T, Lozano PR, Ikeda Y, Iwanaga Y, Hinek A, Minamisawa S, et al. Fibulin-5/DANCE is essential for elastogenesis in vivo. *Nature.* 2002;415:171-5.
28. Mizuno T, Terrence MY, Richard DW, Chris GK, Li R-K. Elastin stabilizes an infarct and preserves ventricular function. *Circulation.* 2005;112:I-81-8.
29. Kitagawa-Sakakida S, Tori M, Li Z, Horiguch K, Izutani H, Matsuda H, et al. Active cell migration in retransplanted rat cardiac allograft during the course of chronic rejection. *J Heart Lung Transplant.* 2000;19:584-90.
30. Tsuda Y, Shimizu T, Yamato M, Kikuchi A, Sasagawa T, Sekiya S, et al. Cellular control of tissue architectures using a three-dimensional tissue fabrication technique. *Biomaterials.* 2007;28:4939-46.

Skeletal myoblast sheet transplantation improves the diastolic function of a pressure-overloaded right heart

Takaya Hoashi, MD,[a] Goro Matsumiya, MD, PhD,[a] Shigeru Miyagawa, MD, PhD,[a] Hajime Ichikawa, MD, PhD,[a] Takayoshi Ueno, MD, PhD,[a] Masamichi Ono, MD, PhD,[a] Atsuhiro Saito, PhD,[a] Tatsuya Shimizu, MD, PhD,[b] Teruo Okano, MD, PhD,[b] Naomasa Kawaguchi, PhD,[c] Nariaki Matsuura, MD, PhD,[c] and Yoshiki Sawa, MD, PhD[a]

Objective: The development of right ventricular dysfunction has become a common problem after surgical repair of complex congenital heart disease. A recent study reported that tissue-engineered skeletal myoblast sheet transplantation improves left ventricular function in patients with dilated and ischemic cardiomyopathy. Therefore myoblast sheet transplantation might also improve ventricular performance in a rat model of a pressure-overloaded right ventricle.

Methods: Seven-week-old male Lewis rats underwent pulmonary artery banding. Four weeks after pulmonary artery banding, myoblast sheet transplantation to the right ventricle was performed in the myoblast sheet transplantation group (n = 20), whereas a sham operation was performed in the sham group (n = 20).

Results: Four weeks after performing the procedure, a hemodynamic assessment with a pressure–volume loop showed a compensatory increase in systolic function in both groups. However, only the myoblast sheet transplantation group showed a significant improvement in the diastolic function: end-diastolic pressure (sham vs myoblast sheet transplantation, 10.3 ± 3.1 vs 5.0 ± 3.7 mm Hg; $P < .001$), time constant of isovolumic relaxation (11.1 ± 2.5 vs 7.6 ± 1.2 ms, $P < .001$), and end-diastolic pressure–volume relationship (16.1 ± 4.5 vs 7.6 ± 2.4/mL, $P < .005$). The right ventricular weight and cell size similarly increased in both groups. A histologic assessment demonstrated significantly suppressed ventricular fibrosis and increased capillary density in the myoblast sheet transplantation group in comparison with those in the sham group. Reverse transcription–polymerase chain reaction demonstrated an increased myocardial gene expression of hepatocyte growth factor and vascular endothelial growth factor in the myoblast sheet transplantation group but not in the sham group.

Conclusions: Skeletal myoblast sheet transplantation improved the diastolic dysfunction and suppressed ventricular fibrosis with increased capillary density in a rat model of a pressure-overloaded right ventricle. This method might become a novel strategy for the myocardial regeneration of right ventricular failure in patients with congenital heart disease.

ET/BS

Because of recent developments in diagnostic methods, the establishment of new surgical techniques, and improvements in perioperative management, patients with complex congenital heart disease (CHD) are today often able to survive to adulthood. However, even after a successful repair, right ventricular (RV) overload remains in some patients, in whom it impairs RV function and influences long-term mortality and morbidity.[1-3] Chronic pressure overload is one of the major risk factors of RV dysfunction. In this situation the right ventricle is hypertrophied and systolic function is initially preserved, whereas diastolic function gradually deteriorates.[4,5] Prolonged exposure to excessive pressure overload results in irreversible RV failure. Clinically, the relationship between progressive fibrosis and RV function must be addressed.[6-8]

Recently, cardiac regeneration therapy has provided a new treatment for end-stage heart failure, and skeletal myoblasts are currently thought to be a potential cell source.[9-11] We developed a novel cell delivery system using temperature-responsive culture dishes,[12] and tissue-engineered cell sheets have been created without any scaffold, which maintains cell–cell interaction and extracellular matrix while avoiding any inflammatory reaction, and with improved cell survival.[13] Skeletal myoblast sheet transplantation (MST) has been shown to improve left ventricular (LV) contractility in several animal models of LV failure.[14-16] Otherwise, it is unclear whether MST can also affect the right ventricle, especially pressure-induced RV dysfunction. Hence this study assessed whether MST could improve RV function in rats after damage caused by pressure overload.

From the Department of Cardiovascular Surgery,[a] Osaka University Graduate School of Medicine, Osaka, Japan; the Institute of Advanced Biomedical Engineering and Science,[b] Tokyo Women's Medical University, Tokyo, Japan; and the Department of Molecular Pathology,[c] Osaka University Graduate School of Allied Health Science, Osaka, Japan.

Received for publication March 17, 2008; revisions received Oct 1, 2008; accepted for publication Feb 2, 2009.

Address for reprints: Yoshiki Sawa, MD, PhD, 2–2 Yamadaoka, Suita, Osaka 565-0871, Japan (E-mail: sawa@surg1.med.osaka-u.ac.jp).

J Thorac Cardiovasc Surg 2009;138:460-7
0022-5223/$36.00

doi:10.1016/j.jtcvs.2009.02.018

Abbreviations and Acronyms

BW = body weight
CFR = coronary flow reserve
EDPVR = end-diastolic pressure–volume relationship
Ees = end-systolic elastance
ESPVR = end-systolic pressure–volume relationship
GAPDH = glyceraldehyde-3-phosphate dehydrogenase
HGF = hepatocyte growth factor
IVS = intraventricular septum
LV = left ventricular
MS = myoblast cell sheet
MST = myoblast sheet transplantation
PA = pulmonary artery
PAB = pulmonary artery banding
PRSW = preload recruitable stroke work
RT-PCR = reverse transcription–polymerase chain reaction
RV = right ventricular
SW = stroke work
VEGF = vascular endothelial growth factor

MATERIALS AND METHODS

Animal Care

All experimental procedures and protocols used in this investigation were reviewed and approved by the institutional animal care and use committee and are in accordance with the National Institutes of Health "Guide for the care and use of laboratory animals" (National Institutes of Health publication no. 85-23, revised 1996).

Creation of Chronic RV Pressure Overload

A rat model of pulmonary artery banding (PAB) was established to create chronic RV pressure overload. Seven-week-old male Lewis rats (180–210 g) were anesthetized with an intraperitoneal injection of ketamine hydrochloride (50 mg/kg) and xylazine (5 mg/kg) and ventilated by using a volume-controlled respirator (2 mL, 60 cycles/min) with room air. A left thoracotomy was performed at the fourth intracostal space, and the main pulmonary artery (PA) was carefully exposed. As previously reported,[17] a 19-gauge injection needle (outer diameter, 1.1 mm) was placed alongside the PA, and a 3-0 polyester suture was tied tightly around the PA and the needle. Next, the needle was rapidly removed, and then a fixed diameter was set for the PA. Thereafter, the thorax was closed in layers, and the ventilator setting was changed (90 cycles/min) for half an hour to reduce the respiratory load.

Skeletal Myoblast Sheet Preparation

Creation of myoblast cell sheets (MSs) with temperature-responsive culture dishes (UpCell; Cellseed, Tokyo, Japan) was done according to previous reports.[14-16] Briefly, skeletal muscle was harvested from the hind legs of 4-week-old syngeneic rats. The purified myoblasts were incubated on 35-mm UpCell dishes at 37°C, with the cell numbers adjusted to 3×10^6 per dish. After 12 to 18 hours, the dishes were moved to a refrigerator set at 20°C and left there for 30 minutes. During that time, the MSs detached spontaneously from the surfaces. Each sheet measured from 10 to 15 mm in diameter.

Skeletal MST

Four weeks after PAB, a second left thoracotomy was performed at the fifth intracostal space after achievement of general anesthesia. After opening the pericardium, the RV anterior wall was exposed. Two MSs were grafted onto each anterior wall of the right ventricle in the MST group (n = 20), or a sham operation was performed in the sham group (n = 20). The pericardium was closed linearly before the thorax was closed to prevent the dislocation of MSs. In addition, age-matched rats that did not undergo surgical intervention were also prepared as a control group (n = 20).

Hemodynamic Study and Data Analysis

Four weeks after the MST or sham operation, 10 rats in each group were anesthetized and ventilated again and were set on the blanket warmer to maintain body temperature. A median sternotomy was performed, and the pericardium was opened carefully to minimize hemorrhaging. A silk thread was placed under the inferior vena cava just above the diaphragm to change the RV preload. After purse-string sutures were attached with 7-0 polypropylene, the conductance catheter (Unique Medical Co, Tokyo, Japan) was inserted through the RV apex toward the pulmonary valve along the longitudinal axis of the RV cavity and then fixed. A Miller 1.4F pressure-tip catheter (SPR-719; Millar Instruments, Houston, Tex) was also inserted from the RV anterior wall and fixed. For better volume measurement, a 1-mm curve was added to the original standard straight conductance catheter to fit the complex RV geometry. The position of the conductance catheter was determined by observing the pressure and segmental volume signals with the appropriate phase relationships. The conductance system and the pressure transducer controller (Integral 3 [VPR-1002], Unique Medical Co) were set as previously reported.[18] Pressure–volume loops and intracardiac electrocardiograms were monitored online, and the conductance, pressure, and intracardiac electrocardiographic signals were analyzed with Integral 3 software (Unique Medical Co).[18]

Under stable hemodynamic conditions, the baseline indices were initially measured, and then the pressure–volume loop was drawn during inferior vena caval occlusion and analyzed (Figure 1). Finally, the conductivity of the sampled blood was measured with a small (0.1 mm) cuvette, and the parallel conductance volume was measured with the hypertonic saline dilution method to obtain the absolute volumes.[19]

The following indices were calculated as the baseline RV function: heart rate, end-systolic pressure, end-diastolic pressure, dP/dtmax, dP/dtmin, and the time constant of isovolumic relaxation (τ). The following relationships were determined by means of pressure–volume loop analysis as load-independent measures of RV function: end-systolic pressure–volume relationship (ESPVR), end-diastolic pressure–volume relationship (EDPVR), and preload recruitable stroke work (PRSW).

The ESPVR is linear, and it can be characterized by a slope (end-systolic elastance [Ees]) and a volume axis intercept (Vo), so that $Pes = Ees(Ves–Vo)$, where Pes and Ves are the end-systolic pressure and volume, respectively.[20]

In contrast, the EDPVR is intrinsically thought to be nonlinear. The relationship between the end-diastolic pressure (Ped) and volume (Ved) can be fitted to the monoexponential, so that $Ped = Po+be^{KvVed}$, where Po is the pressure asymptote (generally close to 0 mm Hg), b is a constant, and Kv is the variable represented as a ventricular stiffness property.[21]

The relationship between ventricular stroke work (SW) and end-diastolic volume (Ved) is represented as PRSW. PRSW is thought to be a suitable parameter of the contractile state and fitted to the following equation: $SW = K(Ved–Vo)$, where K is a constant as a potential measure of intrinsic myocardial performance independent of loading, geometry, and heart rate.[22]

Histopathologic Analysis

The other 10 rats in each group were killed 4 weeks after the sham or MST operation for histologic analysis, reverse transcription–polymerase chain reaction (RT-PCR), and blood sampling. The hearts were quickly removed, and the ventricles were dissected free of atrial tissue and large

ET/BS